J|A|C|S
ARTICLES
Published on Web 09/03/2003

Mechanism of the Alternating Copolymerization of Epoxides and CO_2 Using β-Diiminate Zinc Catalysts: Evidence for a Bimetallic Epoxide Enchainment

David R. Moore, Ming Cheng, Emil B. Lobkovsky, and Geoffrey W. Coates*

Contribution from the Department of Chemistry and Chemical Biology, Baker Laboratory, Cornell University, Ithaca, New York 14853-1301

Received February 5, 2003; E-mail: gc39@cornell.edu

Abstract: A series of zinc β-diiminate (BDI) complexes and their solid-state structures, solution dynamics, and copolymerization behavior with CO_2 and cyclohexene oxide (CHO) are reported. Stoichiometric reactions of the copolymerization initiation steps show that zinc alkoxide and bis(trimethylsilyl)amido complexes insert CO_2, whereas zinc acetates react with CHO. [(BDI-**2**)ZnOMe]$_2$ [(BDI-**2**) = 2-((2,6-diethylphenyl)amido)-4-((2,6-diethylphenyl)imino)-2-pentene] and (BDI-**1**)ZnO^{i}Pr [(BDI-**1**) = 2-((2,6-diisopropylphenyl)amido)-4-((2,6-diisopropylphenyl)imino)-2-pentene] react with CO_2 to form [(BDI-**2**)Zn(μ-OMe)(μ,η^2-O_2COMe)Zn(BDI-**2**)] and [(BDI-**1**)Zn(μ,η^2-O_2CO^{i}Pr)]$_2$, respectively. (BDI-**2**)ZnN(SiMe$_3$)$_2$ inserts CO_2 and eliminates trimethylsilyl isocyanate to give [(BDI-**2**)Zn(μ-OSiMe$_3$)]$_2$. [(BDI-**7**)Zn(μ-OAc)]$_2$ [(BDI-**7**) = 3-cyano-2-((2,6-diethylphenyl)-amido)-4-((2,6-diethylphenyl)imino)-2-pentene] reacts with 1.0 equiv of CHO to yield [(BDI-**7**)Zn(μ,η^2-OAc)-(μ,η^1-OCyOAc)Zn(BDI-**7**)]. Under typical polymerization conditions, rate studies on the copolymerization exhibit no dependence in [CO_2], a first-order dependence in [CHO], and orders in [Zn]$_{tot}$ ranging from 1.0 to 1.8 for [(BDI)ZnOAc] complexes. The copolymerizations of CHO (1.98 M in toluene) and 300 psi CO_2 at 50 °C using [(BDI-**1**)ZnOAc] and [(BDI-**2**)ZnOAc] show orders in [Zn]$_{tot}$ of 1.73 $\pm$ 0.06 and 1.02 $\pm$ 0.03, respectively. We propose that two zinc complexes are involved in the transition state of the epoxide ring-opening event.

Introduction

At present, the predominant source of carbon for raw materials used in the chemical industry is fossil fuels; synthetic plastics account for approximately 7% of worldwide oil and gas consumption.[1] In addition, the current worldwide production of plastics is approximately 150 million tons per year.[1] Because these resources are expected to be depleted in about 80 years,[2] there is significant interest in finding new routes from biorenewable resources to important chemicals, especially biodegradable and recyclable polymers.[3,4]

A current focus of our research is the development of catalysts for the synthesis of polymers from carbon dioxide. Although CO_2 is an ideal synthetic feedstock because it is abundant, inexpensive, nontoxic, and nonflammable, synthetic chemists have had limited success in developing efficient catalytic processes that exploit CO_2 as a raw material.[5−7] Consequently, research efforts in the alternating copolymerization of CO_2 with epoxides to give biodegradable aliphatic polycarbonates[4] continue to grow.[8] A wide variety of recently reported catalytic systems[8−49] convert CO_2 and epoxides into polycarbonates and/or cyclic carbonates. Inoue's discovery of a heterogeneous

(1) Stevens, E. S. *Green Plastics*; Princeton University Press: Princeton, 2002.
(2) Gerngross, T. U.; Slater, S. C. *Sci. Am.* **2000**, *283* (2), 36−41.
(3) Gross, R. A.; Kalra, B. *Science* **2002**, *297*, 803−807.
(4) Okada, M. *Prog. Polym. Sci.* **2002**, *27*, 87−133.
(5) Arakawa, H.; Aresta, M.; Armor, J. N.; Barteau, M. A.; Beckman, E. J.; Bell, A. T.; Bercaw, J. E.; Creutz, C.; Dinjus, E.; Dixon, D. A.; Domen, K.; DuBois, D. L.; Eckert, J.; Fujita, E.; Gibson, D. H.; Goddard, W. A.; Goodman, D. W.; Keller, J.; Kubas, G. J.; Kung, H. H.; Lyons, J. E.; Manzer, L. E.; Marks, T. J.; Morokuma, K.; Nicholas, K. M.; Periana, R.; Que, L.; Rostrup-Nielson, J.; Sachtler, W. M. H.; Schmidt, L. D.; Sen, A.; Somorjai, G. A.; Stair, P. C.; Stults, B. R.; Tumas, W. *Chem. Rev.* **2001**, *101*, 953−996.
(6) For some other leading references, see: (a) Musie, G.; Wei, M.; Subramaniam, B.; Busch, D. H. *Coord. Chem. Rev.* **2001**, *219*, 789−820. (b) Cooper, A. I. *J. Mater. Chem.* **2000**, *10*, 207−234. (c) Leitner, W. *Comptes Rendus Acad. Sci. Ser. II C* **2000**, *3*, 595−600. (d) Bolm, C.; Beckmann, O.; Dabard, O. A. G. *Angew. Chem., Int. Ed.* **1999**, *38*, 907−909. (e) Yin, X. L.; Moss, J. R. *Coord. Chem. Rev.* **1999**, *181*, 27−59. (f) Leitner, W. *Coord. Chem. Rev.* **1996**, *153*, 257−284. (g) Leitner, W. *Angew. Chem., Int. Ed. Engl.* **1995**, *34*, 2207−2221. (h) Jessop, P. G.; Ikariya, T.; Noyori, R. *Chem. Rev.* **1995**, *95*, 259−272.
(7) Gibson, D. H. *Chem. Rev.* **1996**, *96*, 2063−2095.
(8) For reviews on epoxide/CO_2 copolymerizations, see: (a) Darensbourg, D. J.; Holtcamp, M. W. *Coord. Chem. Rev.* **1996**, *153*, 155−174. (b) Super, M. S.; Beckman, E. *J. Trends Polym. Sci.* **1997**, *5*, 236−240. (c) Rokicki, A.; Kuran, W. *J. Macromol. Sci.-Rev. Macromol. Chem. Phys.* **1981**, *C21*, 135−186.
(9) Darensbourg, D. J.; Holtcamp, M. W. *Macromolecules* **1995**, *28*, 7577−7579.
(10) Darensbourg, D. J.; Rainey, P.; Yarbrough, J. C. *Inorg. Chem.* **2001**, *40*, 986−993.
(11) Darensbourg, D. J.; Holtcamp, M. W.; Struck, G. E.; Zimmer, M. S.; Niezgoda, S. A.; Rainey, P.; Robertson, J. B.; Draper, J. D.; Reibenspies, J. H. *J. Am. Chem. Soc.* **1999**, *121*, 107−116.
(12) Darensbourg, D. J.; Wildeson, J. R.; Yarbrough, J. C.; Reibenspies, J. H. *J. Am. Chem. Soc.* **2000**, *122*, 12487−12496.
(13) Darensbourg, D. J.; Wildeson, J. R.; Yarbrough, J. C. *Inorg. Chem.* **2002**, *41*, 973−980.
(14) Super, M. S.; Berluche, E.; Costello, C.; Beckman, E. J. *Macromolecules* **1997**, *30*, 368−372.
(15) Sarbu, T.; Beckman, E. J. *Macromolecules* **1999**, *32*, 6904−6912.
(16) Sarbu, T.; Styranec, T.; Beckman, E. J. *Nature* **2000**, *405*, 165−168.
(17) Darensbourg, D. J.; Lewis, S. J.; Rodgers, J. L.; Yarbrough, J. C. *Inorg. Chem.* **2003**, *43*, 581−589.
(18) Darensbourg, D. J.; Yarbrough, J. C. *J. Am. Chem. Soc.* **2002**, *124*, 6335−6342.
(19) Kruper, W. J.; Dellar, D. V. *J. Org. Chem.* **1995**, *60*, 725−727.

$ZnEt_2/H_2O$ mixture for copolymerization of CO_2 and propylene oxide[50] inspired the development of a number of additional heterogeneous systems.[36−45] Discrete zinc phenoxides developed by Darensbourg[9−12] and ZnO/fluorinated carboxylic acid systems investigated by Beckman[14,15] copolymerize cyclohexene oxide (CHO) and CO_2, exhibiting turnover frequencies (TOF) of approximately 10 h^{-1}. Chromium-based systems, including chromium porphyrins studied by Kruper[19] and Holmes[20,21] and chromium salen complexes reported by Darensbourg,[18] give TOFs of up to 200 h^{-1}. Finally, highly active β-diiminate (BDI) zinc carboxylates and alkoxides designed in our group afford TOFs as high as 2300 h^{-1} for CHO and CO_2 copolymerization (Figure 1).[51−56]

Over the past five years, we have published several reports describing well-defined, single-site BDI zinc complexes as highly active catalysts for the synthesis of biodegradable

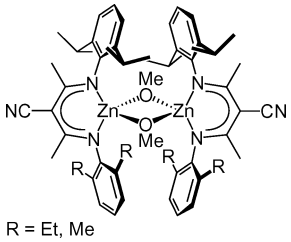

Figure 1. Highly active $[(BDI)Zn(\mu\text{-}OMe)]_2$ complexes for the alternating copolymerization of CHO and CO_2.

Scheme 1. β-Diiminate Zinc Complexes as Catalysts for the Alternating Copolymerization of Cyclohexene Oxide and CO_2

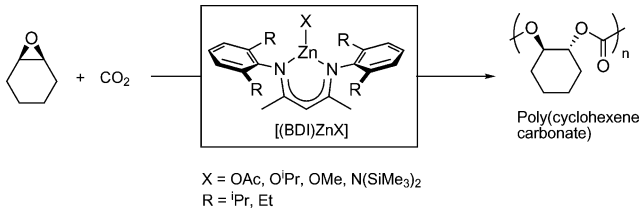

Scheme 2. Catalytic Cycle Illustrating the Alternating Insertion of CHO and CO_2 in the Synthesis of Aliphatic Polycarbonates

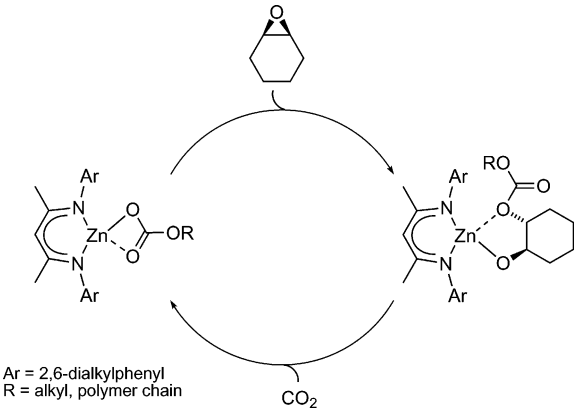

polymers. These include the production of polycarbonates from the alternating copolymerization of carbon dioxide and epoxides (including cyclohexene oxide and propylene oxide) under low temperatures and mild pressures (Schemes 1 and 2),[51−56] heterotactic and syndiotactic poly(lactic acid) from *rac*-lactide and *meso*-lactide, respectively,[57,58] and poly(3-hydroxybutyrate) from β-butyrolactone.[59] Using these systems, narrow polydispersity indices (PDIs) and number average molecular weights (M_n) dictated by monomer-to-initiator ratios are observed, indicative of living polymerizations.[60] Additionally, minor changes in the ligand architecture result in dramatic enhancements in polymerization rates.[54,55]

Homogeneous catalysts have distinct advantages over their heterogeneous counterparts.[61] Single-site homogeneous catalysts are typically of the form L_nMR, containing a readily modifiable organic ligand set (L_n), a catalytically active metal center (M), and a viable initiating group or polymer chain-end (R). These homogeneous catalysts allow for modifications of (1) ligand

(20) Mang, S.; Cooper, A. I.; Colclough, M. E.; Chauhan, N.; Holmes, A. B. *Macromolecules* **2000**, *33*, 303−308.
(21) Stamp, L. M.; Mang, S. A.; Holmes, A. B.; Knights, K. A.; de Miguel, Y. R.; McConvey, I. F. *Chem. Commun.* **2001**, 2502−2503.
(22) Eberhardt, R.; Allmendinger, M.; Luinstra, G. A.; Rieger, B. *Organometallics* **2003**, *22*, 211−214.
(23) Eberhardt, R.; Allmendinger, M.; Rieger, B. *Macromol. Rapid Commun.* **2003**, *24*, 194−196.
(24) Kuran, W.; Listos, T. *Macromol. Chem. Phys.* **1994**, *195*, 977−984.
(25) Dinger, M. B.; Scott, M. J. *Inorg. Chem.* **2001**, *40*, 1029−1036.
(26) Nozaki, K.; Nakano, K.; Hiyama, T. *J. Am. Chem. Soc.* **1999**, *121*, 11008−11009.
(27) Nakano, K.; Nozaki, K.; Hiyama, T. *J. Am. Chem. Soc.* **2003**, *125*, 5501−5510.
(28) Kuran, W.; Listos, T.; Abramczyk, M.; Dawidek, A. *J. Macromol. Sci., Pure Appl. Chem.* **1998**, *A35*, 427−437.
(29) Kim, H. S.; Kim, J. J.; Lee, B. G.; Jung, O. S.; Jang, H. G.; Kang, S. O. *Angew. Chem., Int. Ed.* **2000**, *39*, 4096−4098.
(30) Kim, H. S.; Kim, J. J.; Lee, S. D.; Lah, M. S.; Moon, D.; Jang, H. G. *Chem. Eur. J.* **2003**, *9*, 678−686.
(31) Paddock, R. L.; Nguyen, S. T. *J. Am. Chem. Soc.* **2001**, *123*, 11498−11499.
(32) Shen, Y. M.; Duan, W. L.; Shi, M. *J. Org. Chem.* **2003**, *68*, 1559−1562.
(33) Yano, T.; Matsui, H.; Koike, T.; Ishiguro, H.; Fujihara, H.; Yoshihara, M.; Maeshima, T. *Chem. Commun.* **1997**, 1129−1130.
(34) Yamaguchi, K.; Ebitani, K.; Yoshida, T.; Yoshida, H.; Kaneda, K. *J. Am. Chem. Soc.* **1999**, *121*, 4526−4527.
(35) Kawanami, H.; Ikushima, Y. *Chem. Commun.* **2000**, 2089−2090.
(36) Jung, J. H.; Ree, M.; Chang, T. *J. Polym. Sci., Part A: Polym. Chem.* **1999**, *37*, 3329−3336.
(37) Chen, L. B. *Makromol. Chem. Macromol. Symp.* **1992**, *59*, 75−82.
(38) Ree, M.; Bae, J. Y.; Jung, J. H.; Shin, T. J.; Hwang, Y. T.; Chang, T. *Polym. Eng. Sci.* **2000**, *40*, 1542−1552.
(39) Ree, M.; Bae, J. Y.; Jung, J. H.; Shin, T. J. *Korea Polym. J.* **1999**, *7*, 333−349.
(40) Ree, M.; Bae, J. Y.; Jung, J. H.; Shin, T. J. *J. Polym. Sci., Part A: Polym. Chem.* **1999**, *37*, 1863−1876.
(41) Shen, Z. Q.; Chen, X. H.; Zhang, Y. F. *Macromol. Chem. Phys.* **1994**, *195*, 2003−2011.
(42) Tan, C. S.; Hsu, T. J. *Macromolecules* **1997**, *30*, 3147−3150.
(43) Yang, S. Y.; Fang, X. G.; Chen, L. B. *Polym. Adv. Technol.* **1996**, *7*, 605−608.
(44) Liu, B. Y.; Zhao, X. J.; Wang, X. H.; Wang, F. S. *J. Polym. Sci., Part A: Polym. Chem.* **2001**, *39*, 2751−2754.
(45) Hsu, T. J.; Tan, C. S. *Polymer* **2001**, *42*, 5143−5150.
(46) Zhang, M.; Chen, L. B.; Liu, B.; Yan, Z.; Qin, G.; Li, Z. *Polym. Bull.* **2001**, *47*, 255−260.
(47) Zhang, M.; Chen, L. B.; Qin, G.; Li, Z. M. *Acta Polym. Sin.* **2001**, 422−424.
(48) Zhang, M.; Chen, L. B.; Qin, G.; Liu, B.; Yan, Z.; Li, Z. *J. Appl. Polym. Sci.* **2003**, *87*, 1123−1128.
(49) Wang, S. J.; Du, L. C.; Zhao, X. S.; Meng, Y. Z.; Tjong, S. C. *J. Appl. Polym. Sci.* **2002**, *85*, 2327−2334.
(50) Inoue, S.; Koinuma, H.; Tsuruta, T. *J. Polym. Sci., Part B: Polym. Lett.* **1969**, *7*, 287−292.
(51) Cheng, M.; Lobkovsky, E. B.; Coates, G. W. *J. Am. Chem. Soc.* **1998**, *120*, 11018−11019.
(52) Coates, G. W.; Cheng, M. (Cornell Research Foundation), U.S. Pat. 6133402, 2002 (*Chem Abstr.* **2000**, *132*, 152332).
(53) Cheng, M.; Darling, N. A.; Lobkovsky, E. B.; Coates, G. W. *Chem. Commun.* **2000**, 2007−2008.
(54) Cheng, M.; Moore, D. R.; Reczek, J. J.; Chamberlain, B. M.; Lobkovsky, E. B.; Coates, G. W. *J. Am. Chem. Soc.* **2001**, *123*, 8738−8749.
(55) Moore, D. R.; Cheng, M.; Lobkovsky, E. B.; Coates, G. W. *Angew. Chem., Int. Ed.* **2002**, *41*, 2599−2602.
(56) Allen, S. D.; Moore, D. R.; Lobkovsky, E. B.; Coates, G. W. *J. Am. Chem. Soc.* **2002**, *124*, 14284−14285.
(57) Cheng, M.; Attygalle, A. B.; Lobkovsky, E. B.; Coates, G. W. *J. Am. Chem. Soc.* **1999**, *121*, 11583−11584.
(58) Chamberlain, B. M.; Cheng, M.; Moore, D. R.; Ovitt, T. M.; Lobkovsky, E. B.; Coates, G. W. *J. Am. Chem. Soc.* **2001**, *123*, 3229−3238.
(59) Rieth, L. R.; Moore, D. R.; Lobkovsky, E. B.; Coates, G. W. *J. Am. Chem. Soc.* **2002**, *124*, 15239−15248.
(60) Matyjaszewski, K.; Mueller, A. H. E. *Polym. Prepr. (American Chemical Society, Division of Polymer Chemistry)* **1997**, *38* (1), 6−9.
(61) Coates, G. W. *Chem. Rev.* **2000**, *100*, 1223−1252.

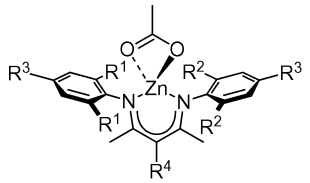

Ligand	R^1	R^2	R^3	R^4
(BDI-**1**)H	^{i}Pr	^{i}Pr	H	H
(BDI-**2**)H	Et	Et	H	H
(BDI-**3**)H	Me	Me	H	H
(BDI-**4**)H	Et	Et	^{t}Bu	H
(BDI-**5**)H	^{i}Pr	Et	H	H
(BDI-**6**)H	^{i}Pr	^{i}Pr	^{t}Bu	H
(BDI-**7**)H	Et	Et	H	CN

Figure 2. β-Diiminate zinc acetate complexes.

electronics and sterics, (2) labile metal centers, and (3) viable initiating groups. Mechanistic information can be retrieved from a system designed with a single-site catalyst, whereas the presence of multiple active sites makes obtaining this information difficult. Therefore, it has been our goal to develop single-site BDI zinc complexes, which are specifically designed to possess a permanent ligand on the active metal center, as well as an initiating group, which serves to mimic the putative propagating species of the polymer chain.

Our recent findings suggested that the enhanced rates of the unsymmetrical isopropyl and ethyl/methyl-substituted catalysts[55] (see Figure 1) could be informative regarding the mechanism in the copolymerization of CHO and CO_2 (see Scheme 2). The symmetrically substituted complexes [(BDI-**1**)ZnOAc] and [(BDI-**2**)ZnOAc] (Figure 2) are effective catalysts for the alternating copolymerization of CHO and CO_2. However, complexes that do not possess adequate steric bulk in the ortho positions of the *N*-aryl ring exist as highly unreactive dimeric species (Figure 3). Conversely, bulky substituents yield predominantly monomeric complexes in solution that also impede catalysis. Therefore, we synthesized and investigated a variety of zinc complexes in the regime of activity between unreactive tightly bound dimers and monomers. Herein we report solution studies, stoichiometric enchainment events, copolymerization data, and rate studies for the alternating copolymerization of CO_2 and CHO. We propose a detailed mechanism, in which the rate-determining step is a bimetallic epoxide enchainment event.

Results and Discussion

Synthesis and Solid-State Structures of Zinc Catalysts. Previous results showed that subtle ligand modifications produce dramatic effects on catalytic activity.[54,55] For instance, complexes with inadequate steric bulk at the four *N*-aryl ortho positions, such as methyl substituents ([(BDI-**3**)ZnOAc]; Figure 2), fail to afford polymerization activity. However, complexes containing different *N*-aryl substituents (e.g., 2,6-diisopropylphenyl/2,6-dimethylphenyl) and an electron-withdrawing cyano substituent on the ligand generate the most active catalysts for the alternating copolymerization of CHO and CO_2 (see Figure 1).[55] To probe the highly sensitive structure−activity relationships in these systems, we synthesized zinc acetate complexes of varying bulk in the *N*-aryl positions (see Figure 2).

Reaction of the β-diimine ligands with $ZnEt_2$ affords the monomeric (BDI)ZnEt complexes,[54] which can be cleanly converted to the zinc acetate analogues in up to 87% yield by protonating the zinc ethyl moiety with 1.0 equiv of acetic acid at 0 °C.[56] As with [(BDI)ZnOAc] complexes ligated by **1**−**2**,[51,54] complexes ligated by **3**−**7** are dimeric in the solid state. X-ray analysis of [(BDI-**3**)Zn(μ-OAc)]$_2$ shows a dimer with four-coordinate zinc centers containing bridging η^2-acetates between *syn-syn* and *syn-anti* geometry.[62] There are close interactions between Zn(2) and O(1) (2.497 Å) as well as between Zn(1) and O(4) (3.049 Å). The molecular structures of [(BDI-**4**)Zn(μ,η^2-OAc)]$_2$ and [(BDI-**6**)Zn(μ,η^2-OAc)]$_2$ are dimers isostructural to [(BDI-**2**)Zn(μ,η^2-OAc)]$_2$ and [(BDI-**1**)Zn(μ,η^2-OAc)]$_2$, respectively.[62] [(BDI-**5**)Zn(μ,η^2-OAc)]$_2$ crystallizes in an *anti* fashion (Figure 4). The bridging acetates in [(BDI-**5**)Zn(μ,η^2-OAc)]$_2$ are between *syn-syn* and *syn-anti* geometry, similar to [(BDI-**2**)Zn(μ,η^2-OAc)]$_2$, Additionally, the Zn··Zn separation is 4.14 Å, which is intermediate between the 4.24 and 3.94 Å Zn··Zn separations of [(BDI-**1**)Zn(μ,η^2-OAc)]$_2$ and [(BDI-**2**)Zn(μ,η^2-OAc)]$_2$, respectively. [(BDI-**7**)Zn(μ,η^2-OAc)]$_2$ also crystallizes as a dimer (Figure 5) with a Zn··Zn separation of 3.85 Å, about 0.1 Å shorter than the Zn··Zn separation for [(BDI-**2**)Zn(μ,η^2-OAc)]$_2$. The bridging acetates are between *syn-syn* and *anti-syn* geometries, comparable to [(BDI-**2**)Zn(μ,η^2-OAc)]$_2$. Crystal data and structure refinements are provided in Table 1.

Monomer−Dimer Equilibria of Zinc Acetate and Alkoxide Complexes. [(BDI-**1**)ZnOAc] and related zinc complexes are single-site catalysts and therefore provide an excellent opportunity to model the dynamic behavior of related catalytic intermediates in solution. The ^{1}H NMR spectrum of [(BDI-**1**)ZnOAc] in toluene-d_8 ($[Zn]_{tot} = 1.0 \times 10^{-2}$ M) exhibits two sets of resonances, the relative intensities of which vary with concentration. The set that becomes more intense as concentration decreases was assigned to the monomeric species.[62] The monomer predominates in solution at typical copolymerization conditions (50 °C, $[Zn]_{tot} = 1.0 \times 10^{-2}$ M). Coordinating solvents such as tetrahydrofuran (THF) do not significantly affect the equilibrium, suggesting that the acetate of the monomer exists in the η^2 form. In contrast to [(BDI-**1**)ZnOAc], the ^{1}H NMR spectrum of [(BDI-**2**)ZnOAc] exhibits exclusively one set of resonances in toluene-d_8 ($[Zn]_{tot} = 1.0 \times 10^{-2}$ M) from 20 to 100 °C, consistent with only a dimer in solution. Methine resonances due to dimeric and monomeric species are observed from 4.6 to 4.8 ppm and 4.9 to 5.0 ppm, respectively. [(BDI-**3**)ZnOAc], [(BDI-**4**)ZnOAc], [(BDI-**5**)ZnOAc], and [(BDI-**7**)ZnOAc] each show one set of peaks in benzene-d_6, including a single methine backbone resonance for [(BDI-**3**)ZnOAc], [(BDI-**4**)ZnOAc], and [(BDI-**5**)ZnOAc] between 4.6 and 4.8 ppm, consistent with the dimeric complex. However, [(BDI-**4**)ZnOAc], [(BDI-**5**)ZnOAc], and [(BDI-**7**)ZnOAc] are fluxional dimers on the ^{1}H NMR time scale, characterized by broader resonances at 20 °C which become more well defined at 60 °C. Similar to that of [(BDI-**1**)ZnOAc], ^{1}H NMR spectroscopy of [(BDI-**6**)ZnOAc] reveals a monomer/dimer equilibrium at room temperature ($[Zn]_{tot} = 2.1 \times 10^{-2}$ M in toluene-d_8), which becomes predominantly monomer at 80 °C.[62]

The monomer/dimer equilibrium of [(BDI-**1**)ZnOAc]$_2$, (2 [(BDI-**1**)ZnOAc] ⇌ [(BDI-**1**)ZnOAc]$_2$), was studied between −80 and 100 °C using ^{1}H NMR spectroscopy (400 MHz) in toluene-d_8 ($[Zn]_{tot} = 2.2 \times 10^{-2}$ M; 20 °C, $K_{eq} = 207$ M^{-1}; 50 °C, $K_{eq} = 35$ M^{-1}). From the plot of ln K_{eq} versus $1/T$,[62] a ΔH and ΔS of -10.8 ± 0.1 kcal/mol and -26.3 ± 0.3 eu are found from the slope and intercept. For this solution, the complex is predominantly dimer between −80 and −20 °C;

(62) See Supporting Information.

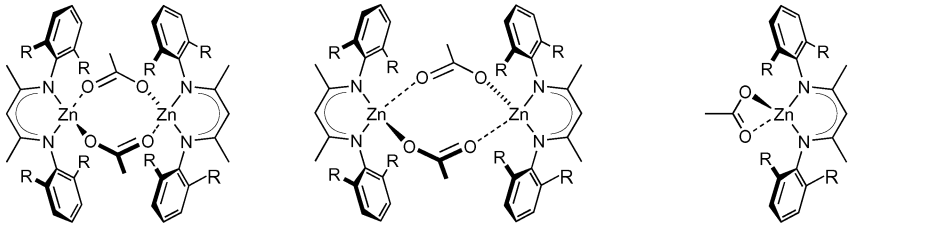

Figure 3. Tightly bound dimers and monomers show poor catalytic activity for the alternating copolymerization of CHO and CO_2. Loosely bound dimers are highly reactive catalysts (R = alkyl).

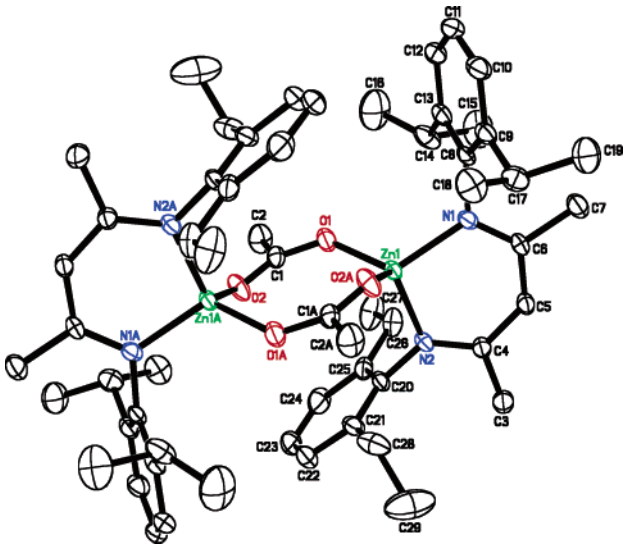

Figure 4. ORTEP drawing of [(BDI-**5**)Zn(μ,η^2-OAc)]$_2$ (non-hydrogen atoms) with thermal ellipsoids drawn at the 40% probability level. Selected bond lengths (Å) and bond angles (deg): Zn(1)−N(1) 1.971(2), Zn(1)−N(2) 1.962(2), Zn(1)−O(1) 1.959(2), Zn(1)−O(2A) 1.947(2), O(1)−C(1) 1.262(2), O(2)−C(1) 1.233(4), O(1)−Zn(1)−O(2A) 111.63(9), N(1)−Zn-(1)-N(2) 98.7(1), N(1)−Zn(1)−O(2A) 108.09(9), N(2)−Zn(1)-O(1) 107.45-(8), C(1)−O(1)−Zn(1) 137.7(2), O(1)−C(1)−O(2) 127.1(2).

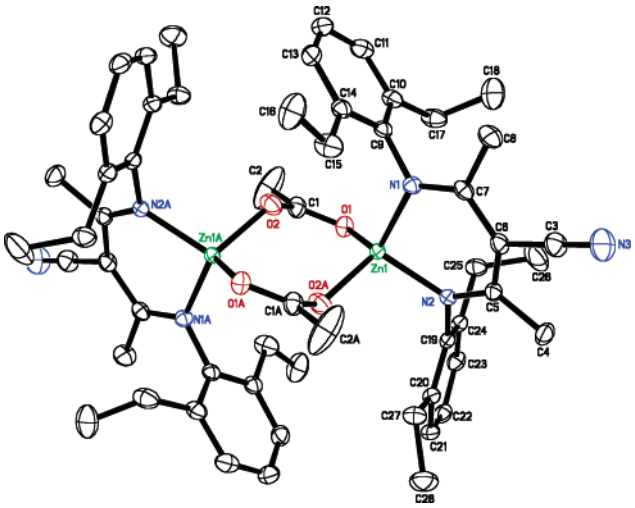

Figure 5. ORTEP drawing of [(BDI-**7**)Zn(μ,η^2-OAc)]$_2$ (non-hydrogen atoms) with thermal ellipsoids drawn at the 40% probability level. Selected bond lengths (Å) and bond angles (deg): Zn(1)−N(1) 1.979(2), Zn(1)−N(2) 1.970 (2), Zn(1)−O(1) 1.962 (1), Zn(1)−O(2A) 1.974(2), O(1)−C(1) 1.252(3), O(2)−C(1) 1.264(3), O(1)−Zn(1)−O(2A) 107.07(7), N(1)−Zn-(1)−N(2) 97.00(6), N(1)−Zn(1)−O(1) 111.79(6), N(2)−Zn(1)−O(2A) 104.65(7), C(1)−O(1)−Zn(1) 111.9(1), O(1)−C(1)−O(2) 122.5(2).

from approximately −20 to 80 °C the complex is in both dimer and monomer forms; and at 100 °C only the monomer is present. Upon cooling from −40 to −80 °C, a broad shift at 0.8 ppm that was assigned to the internal methyl groups of the isopropyl substituents on the ligands coalesces at approximately −60 °C and reemerges at −80 °C. We believe this is due to site exchange between a C_{2h} symmetric dimer species through a D_{2h} symmetric dimer intermediate.[62]

Our previous studies on BDI zinc alkoxides show that (BDI-**1**)ZnO^{i}Pr is predominantly monomeric in benzene-d_6 at room temperature but exhibits a monomer/dimer equilibrium at lower temperatures.[59] Chisholm observed (BDI-**1**)ZnO^{t}Bu and (BDI-**1**)ZnOSiPh$_3$·THF to be monomeric in both the solid state and in solution, and (BDI-**1**)ZnOSiPh$_3$·THF shows a temperature-dependent reversible dissociation of THF.[63,64] We have found that [(BDI-**2**)Zn(μ-O^{i}Pr)]$_2$ and [(BDI-**2**)Zn(μ-OMe)]$_2$ are both dimeric at room temperature ([Zn]$_{tot}$ = 5.6 × 10^{-2} M), but they participate in a slow exchange reaction to produce a mixed dimer over the course of days.[59] Because both methoxide and acetate complexes exist at least partially as monomeric species in benzene solution, we explored combined solutions of these compounds to access the relative stability of dimers of acetate (eight-membered ring), methoxide (four-membered ring), and mixed (six-membered ring) species. The relative energies of such species provide useful insight into potential catalytic ground states during CO_2/epoxide polymerizations. Equimolar amounts of [(BDI-**2**)Zn(μ-OMe)]$_2$ and [(BDI-**2**)Zn(μ,η^2-OAc)]$_2$ were dissolved in toluene at room temperature ([Zn]$_{tot}$ = 1.2 × 10^{-1} M). After 1 h of stirring, ^{1}H NMR spectroscopy revealed a new compound in quantitative yield (Scheme 3). Following crystallization, X-ray diffraction revealed the molecular structure to be a mixed dimer of the form [(BDI-**2**)Zn(μ-OMe)(μ,η^2-OAc)-Zn(BDI-**2**)] (Figure 6; Table 1), suggesting that the six-membered ring mixed dimer exhibits greater stability than do either of the homodimers. The acetate bridge exhibits a *syn-syn* geometry, with a Zn··Zn separation of 3.38 Å.

Therefore, as the *N*-aryl ring substituents on the zinc acetate complexes become more sterically congested, two general trends are observed: (1) the Zn··Zn separations in the solid state increase and (2) the aggregatory state in solution changes from a tightly bound dimer to a fluxional, loosely bound dimer, and finally to a monomer/dimer equilibrium (see Table 2; Figure 3).

(63) Chisholm, M. H.; Gallucci, J.; Phomphrai, K. *Inorg. Chem.* **2002**, *41*, 2785−2794.
(64) Chisholm, M. H.; Huffman, J. C.; Phomphrai, K. *J. Chem. Soc., Dalton Trans.* **2001**, 222−224.

Table 1. Crystal Data and Structure Refinement Parameters

	[(BDI-**5**)-(μ,η^2-OAc)]$_2$	[(BDI-**7**)Zn-(μ,η^2-OAc)]$_2$	[(BDI-**2**)Zn(μ-OMe)-(μ,η^2-OAc)Zn(BDI-**2**)]	[(BDI-**2**)Zn(μ-OMe)-(μ,η^2-O_2COMe)Zn(BDI-**2**)]	[(BDI-**1**)Zn-(μ,η^2-O_2CO^{i}Pr)]$_2$	[(BDI-**2**)Zn-(μ-OSiMe$_3$)]$_2$	[(BDI-**7**)Zn(μ,η^2OAc)-(μ,η^1-OCyOAc)Zn[(BDI-**7**)]
emp form.	$C_{29}H_{40}N_2O_2Zn$	$C_{28}H_{35}N_3O_2Zn\cdot 0.5C_7H_8$	$C_{53}H_{72}N_4O_3Zn_2$	$C_{53}H_{72}N_4O_4Zn_2\cdot C_7H_8$	$C_{66}H_{96}N_4O_6Zn_2\cdot C_6H_6$	$C_{28}H_{42}N_2OSiZn\cdot 0.5C_7H_8$	$C_{124}H_{158}N_{12}O_{10}Zn_4\cdot C_6H_6\cdot 0.5C_6H_{12}\cdot 0.5C_4H_8O$
form. wt	514.00	557.03	943.89	1052.02	1250.32	562.16	2394.34
temp [K]	173(2)	173(2)	173(2)	173(2)	173(2)	173(2)	173(2)
λ [Å]	0.71073	0.71073	0.71073	0.71073	0.71073	0.71073	0.71073
cryst system	triclinic	triclinic	monoclinic	monoclinic	monoclinic	orthorhombic	triclinic
space group	$P\bar{1}$	$P\bar{1}$	$P2_1/n$	$P2_1/c$	$C2$	$Aba2$	$P\bar{1}$
a (Å)	11.7387(4)	10.0930(5)	13.375(1)	13.5383(2)	17.70(3)	19.8633(8)	16.912(4)
b (Å)	11.8892(4)	12.9843(7)	16.907(1)	16.8540(3)	19.44(3)	17.2928(8)	17.554(4)
c (Å)	12.2015(5)	13.4344(7)	22.331(2)	24.8141(1)	11.73(2)	17.5338(8)	24.490(6)
α (deg)	115.718(2)	62.580(1)	90	90	90	90	101.955(8)
β (deg)	105.019(2)	74.139(1)	95.531(2)	93.154(1)	121.66(3)	90	101.881(6)
γ (deg)	102.599(3)	69.807(1)	90	90	90	90	90.558(6)
V [Å^3]	1370.70(9)	1452.85(13)	5026.2(6)	5653.4(1)	3435(8)	6022.7(5)	6950(3)
Z	2	2	4	4	2	8	2
ρ_{calc} [Mg/m^3]	1.245	1.273	1.247	1.236	1.209	1.240	1.144
μ (Mo Kα) [mm^{-1}]	0.923	0.871	0.999	0.896	0.750	0.881	0.739
F(000)	548	582	2008	2240	1340	2376	2518
cryst size [mm]	0.40 × 0.30 × 0.05	0.30 × 0.15 × 0.10	0.40 × 0.20 × 0.20	0.50 × 0.30 × 0.05	0.30 × 0.20 × 0.10	0.20 × 0.15 × 0.10	0.30 × 0.20 × 0.05
θ range (deg)	2.76 to 28.28	2.17 to 33.14	1.51 to 28.37	1.46 to 23.26	2.04 to 18.83	2.32 to 26.37	1.31 to 23.26
index ranges	$-15<=h<=15$ $-15<=k<=14$ $-16<=l<=15$	$-14<=h<=14$ $-19<=k<=18$ $-18<=l<=19$	$-16<=h<=16$ $-22<=k<=22$ $-24<=l<=29$	$-14<=h<=15$ $-14<=k<=18$ $-27<=l<=27$	$-16<=h<=15$ $-17<=k<=17$ $-10<=l<=10$	$-24<=h<=23$ $-21<=k<=18$ $-21<=l<=21$	$-18<=h<=18$ $-19<=k<=19$ $-26<=l<=27$
data collected	10033	19971	31651	24119	7362	18561	34202
unique data	5409	9206	11542	8081	2696	6122	19135
R_{int}	0.0272	0.0302	0.0498	0.0792	0.0606	0.0465	0.0476
GOF	1.041	1.058	0.867	1.005	1.033	1.046	1.011
final R indices [$I > 2\sigma(I)$]	$R_1 = 0.0458$ wR2 = 0.1214	$R_1 = 0.0447$ wR2 = 0.1102	$R_1 = 0.0400$ wR2 = 0.0918	$R_1 = 0.0527$ wR2 = 0.1121	$R_1 = 0.0607$ wR2 = 0.1321	$R_1 = 0.0409$ wR2 = 0.0903	$R_1 = 0.0698$ wR2 = 0.2048
R indices (all data) [$I > 2\sigma(I)$]	$R_1 = 0.0585$ wR2 = 0.1279	$R_1 = 0.0618$ wR2 = 0.1179	$R_1 = 0.0846$ wR2 = 0.1115	$R_1 = 0.0918$ wR2 = 0.1299	$R_1 = 0.0938$ wR2 = 0.1606	$R_1 = 0.0651$ wR2 = 0.1007	$R_1 = 0.1308$ wR2 = 0.2427
$\rho_{min} - \rho_{max}$ [e·Å^{-3}]	1.282 and −0.876	0.919 and −0.659	0.446 and −0.354	0.564 and −0.533	1.357 and −0.445	0.428 and −0.305	0.951 and −0.341

Table 2. Copolymerization of CO_2 and Cyclohexene Oxide Using β-Diiminate (BDI) Zinc Complexes[a]

complex	Zn··Zn separation (Å)[b]	solution structure[c]	reaction time (h)	TON[d]	TOF (h^{-1})[e]	% carbonate linkages[f]	M_n (×10^{-3}) (GPC)[g]	M_w/M_n
(BDI-**1**)ZnN(SiMe$_3$)$_2$	NA[h]	M	0.5	172	345	94	25.5	1.10
(BDI-**2**)ZnN(SiMe$_3$)$_2$	NA[h]	M	0.5	179	358	97	25.6	1.16
(BDI-**1**)ZnN(SiMe$_3$)$_2$ + (BDI-**2**)ZnN(SiMe$_3$)$_2$[i]	NA[h]	M	0.5	329	658	94	40.8	1.17
[(BDI-**1**)ZnOAc]$_2$	4.2448(7)	M/D	0.5	180	360	95	15.8	1.11
[(BDI-**2**)ZnOAc]$_2$	3.941(1)	D	0.5	216	431	97	17.3	1.15
[(BDI-**3**)ZnOAc]$_2$	3.8071(6)	D	0.5	0	0	NA[h]	NA[h]	NA[h]
[(BDI-**4**)ZnOAc]$_2$	4.0948(6)	D[j]	0.5	311	622	98	24.9	1.17
[(BDI-**5**)ZnOAc]$_2$	4.1392(7)	D[j]	0.5	364	729	99	23.3	1.15
[(BDI-**6**)ZnOAc]$_2$	4.1804(9)	M/D	5	140	28	51	85.8/7.26[k]	1.43/1.08[k]
[(BDI-**7**)ZnOAc]$_2$	3.8486(4)	D[j]	0.33	306	917	90	17.9	1.15

[a] All reactions were performed in neat cyclohexene oxide (CHO) with [monomer]:[Zn] = 1000:1 (10 mM in Zn) at 50 °C. [b] Zn··Zn separations from X-ray crystallographic studies. See Supporting Information for crystal data and structure refinement. [c] M = monomeric species; D = dimeric species; M/D = both monomer and dimer present. Solution dynamic studies performed in C_6D_6 at room temperature (10 mM in Zn). [d] TON = turnover number; moles of CHO consumed per mole of zinc. [e] TOF = turnover frequency; moles of CHO consumed per mole of zinc per hour. [f] Calculated by integration of methine resonances in ^{1}H NMR of polymer ($CDCl_3$, 300 MHz). [g] Determined by gel-permeation chromatography (GPC), calibrated with polystyrene standards in tetrahydrofuran. [h] Not applicable. [i] Equimolar ratios of (BDI-**1**)ZnN(SiMe$_3$)$_2$ and (BDI-**2**)ZnN(SiMe$_3$)$_2$. [j] At room temperature, broad dimeric resonances are observed, indicating a fluxional process on the NMR time scale. [k] A bimodal distribution is observed by GPC.

Examination of CHO and CO_2 Enchainment Steps Using Model Compounds. The single-site structure of BDI zinc complexes allows detailed study of the copolymerization enchainment steps through stoichiometric reactions with CO_2 or CHO. The catalyst must react with one of the two monomers to effectively initiate the copolymerization (see Scheme 2). As expected, zinc alkoxides react with CO_2 (Scheme 4). For example, [(BDI-**2**)Zn(μ-OMe)]$_2$[54] inserted 1 equiv of carbon dioxide per dimeric complex when pressurized with 100 psi CO_2 in toluene at 50 °C. X-ray analysis revealed the molecular structure to be [(BDI-**2**)Zn(μ-OMe)(μ,η^2-O_2COMe)Zn(BDI-**2**)] (Figure 7; Table 1), a dimeric compound with a distorted tetrahedral geometry around zinc and a planar six-membered ring at the core of the molecule. [(BDI-**2**)Zn(μ-OMe)(μ,η^2-O_2-COMe)Zn(BDI-**2**)] is isostructural to [(BDI-**2**)Zn(μ-OMe)-(μ,η^2-OAc)Zn(BDI-**2**)] and is further evidence supporting the

Scheme 3. Solution Behavior of [(BDI-**2**)]Zn(μ-OMe)]$_2$ and [(BDI-**2**)Zn(μ-OAc)]$_2$; Exclusive Product Is [(BDI-**2**)Zn(μ-OMe)(μ-OAc)Zn(BDI-**2**)]

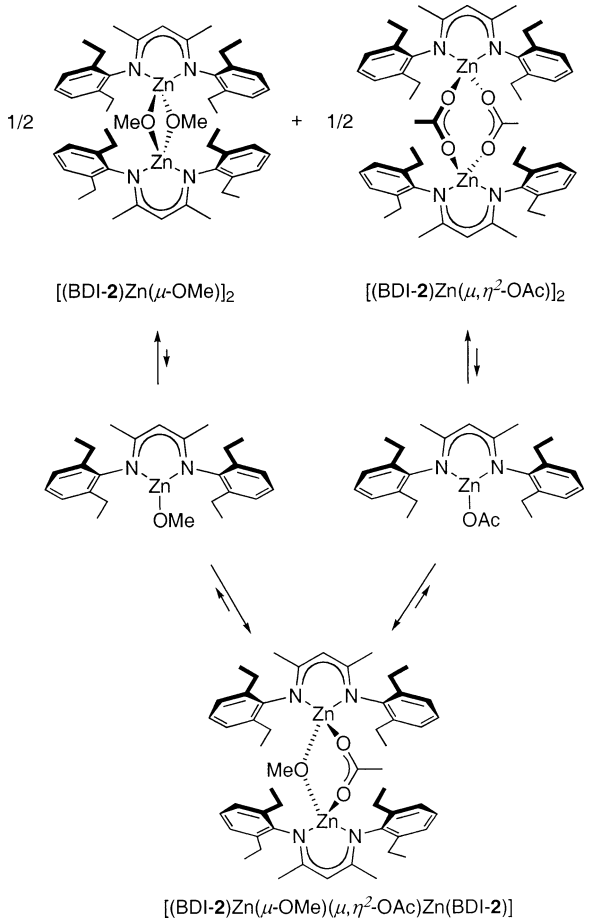

thermodynamic stability of the six-membered dimeric species compared to that of the four-membered zinc alkoxide and eight-membered zinc acetate dimers.

Interestingly, when a toluene solution of the bulkier, monomeric [(BDI-**1**)ZnO^{i}Pr] was pressurized with 100 psi CO_2 at 50 °C, clear blocks instantly crystallized from solution. X-ray analysis revealed the molecular structure to be [(BDI-**1**)Zn(μ,η^2-O_2CO^iPr)]$_2$ (Figure 8; Table 1).[65] Thus, CO_2 is inserted into each zinc isopropoxide bond; dimerization through bridging carbonate groups forms a molecule containing distorted tetrahedral zinc centers. The bridging carbonates adopt a *syn-syn* geometry, creating a planar eight-membered ring at the core of the molecule. The Zn··Zn separation is 4.01 Å, which is considerably shorter than the 4.24 Å Zn··Zn separation observed in [(BDI-**1**)Zn(μ,η^2-OAc)]$_2$. [(BDI-**1**)Zn(μ,η^2-O_2CO^iPr)]$_2$ is nearly isostructural to [(BDI-**1**)Zn(μ,η^2-OAc)]$_2$, and we believe that these related species closely mimic the putative propagating species of the copolymerization reaction. Additionally, we propose that CO_2 insertion occurs into a monometallic zinc alkoxide species due to the rapid reaction of CO_2 with monomeric, three-coordinate (BDI-**1**)ZnO^{i}Pr although we cannot exclude alternate mechanisms.[66]

The alkoxides are excellent models for the catalytic species that enchain CO_2; however, the zinc bis(trimethylsilyl)amido

(65) The non-carbon atoms and carbon atoms of [(BDI-**1**)Zn(μ,η^2-O_2CO^iPr)]$_2$ were refined anisotropically and isotropically, respectively.

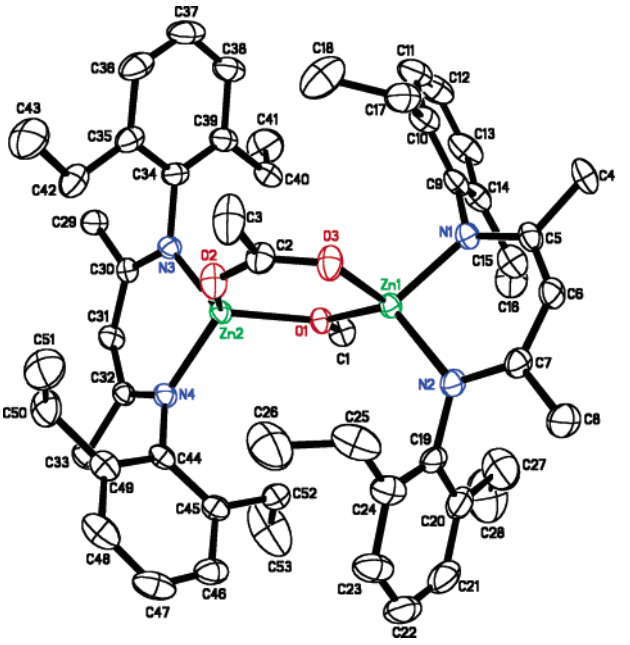

Figure 6. ORTEP drawing of [(BDI-**2**)Zn(μ-OMe)(μ,η^2-OAc)Zn(BDI-**2**)] (non-hydrogen atoms) with thermal ellipsoids drawn at the 40% probability level. Selected bond lengths (Å) and bond angles (deg): Zn(1)−N(1) 1.980(2), Zn(1)−N(2) 1.983(2), Zn(1)−O(1) 1.930(2), Zn(1)−O(3) 1.999(2), C(2)−O(2) 1.251(3), C(2)−O(3) 1.251(3), Zn(2)−O(1) 1.958(2), Zn(2)−O(2) 1.956(2), N(1)−Zn(1)−N(2) 97.51(9), O(1)−Zn(1)−O(3) 102.18(8), N(1)−Zn(1)−O(1) 118.07(8), N(1)−Zn(1)−O(3) 106.76(9), Zn(1)−O(1)−Zn(2) 120.84(9), C(2)−O(3)−Zn(1) 132.6(2), O(2)−C(2)−O(3) 126.2(3), C(2)−O(2)−Zn(2) 133.8(2).

initiators do not adequately imitate the structure of a growing polymer chain. Despite this distinction, they are viable initiators (see Scheme 4). Pressurizing a toluene solution of (BDI-**2**)ZnN(SiMe$_3$)$_2$ at 50 °C with 100 psi CO_2 overnight resulted in the formation of a white precipitate. Analysis of the mother liquor by ^{1}H NMR spectroscopy showed the presence of trimethylsilyl isocyanate. After recrystallization, X-ray analysis revealed a molecular structure corresponding to [(BDI-**2**)Zn(μ-OSiMe$_3$)]$_2$ (Figure 9; Table 1). The structure shows a bridged siloxide dimer with a distorted tetrahedral geometry around each zinc. The Zn−O bonds are 1.98 and 2.03 Å, the Zn−N bonds are 1.96 and 2.05 Å, and the O−Si bond is 1.64 Å. We propose that CO_2 inserts into the zinc amido bond and is followed by migration of a trimethylsilyl group and loss of trimethylsilyl isocyanate.[53,54,67] We are currently investigating why this catalytically active zinc siloxide complex does not further react with CO_2 and crystallize as a six- or eight-membered ring carbonate dimer. Finally, (BDI-**1**)ZnO^{i}Pr and (BDI-**1**)ZnN(SiMe$_3$)$_2$ do not react with CHO, indicating that the BDI zinc alkoxides and bis(trimethylsilyl)amido complexes react readily with only CO_2.

Because zinc alkoxides initiate the copolymerization by reaction with CO_2, zinc acetate compounds, mimics for the putative carbonate species, were expected to complete the

(66) On the basis of their high reactivity, we expect propagating (BDI-**1**)Zn alkoxides to be three-coordinate or weakly chelated, four-coordinate monomeric species. We are currently studying the nature of the zinc alkoxide intermediates in the polymerization and believe that their coordination in solution is highly dependent on ligand sterics and electronics. Furthermore, kinetic studies on the reaction of CO_2 with (BDI-**1**)ZnO^{i}Pr and other BDI zinc alkoxide complexes are underway.

(67) Chisholm has synthesized (BDI-**1**)ZnO(CO)N^{i}Pr$_2$ from (BDI-**1**)ZnN^{i}Pr$_2$ and CO_2 (see ref 63) but found no activity for CO_2/epoxide copolymerization, presumably because rearrangement to the zinc isopropoxide could not occur.

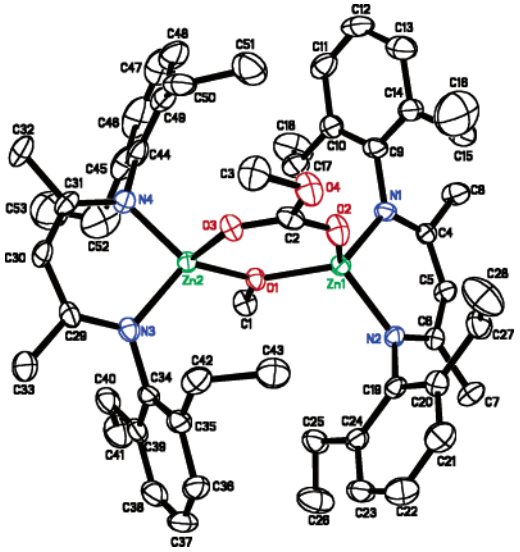

Figure 7. ORTEP drawing of [(BDI-**2**)Zn(μ-OMe)(μ,η^2-O_2COMe)Zn(BDI-**2**)] (non-hydrogen atoms) with thermal ellipsoids drawn at the 40% probability level. Selected bond lengths (Å) and bond angles (deg): Zn(1)−N(1) 1.976(3), Zn(1)−N(2) 1.965(3), Zn(1)−O(1) 1.947(3), Zn(1)−O(2) 1.954(3), Zn(2)−O(1) 1.922(3), Zn(2)−O(3) 2.004(3), C(2)−O(4) 1.350(5), C(2)−O(2) 1.250(6), N(1)−Zn(1)−N(2) 98.1(1), O(1)−Zn(1)−O(2) 103.0(1), N(1)−Zn(1)−O(1) 117.1(1), N(2)−Zn(1)−O(2) 112.5(1), Zn(1)−O(1)−Zn(2) 122.4(2), C(2)−O(2)−Zn(1) 132.0(3), O(2)−C(2)−O(3) 128.5(5), C(2)−O(3)−Zn(2) 133.0(3).

Scheme 4. Insertion Reactions of CO_2

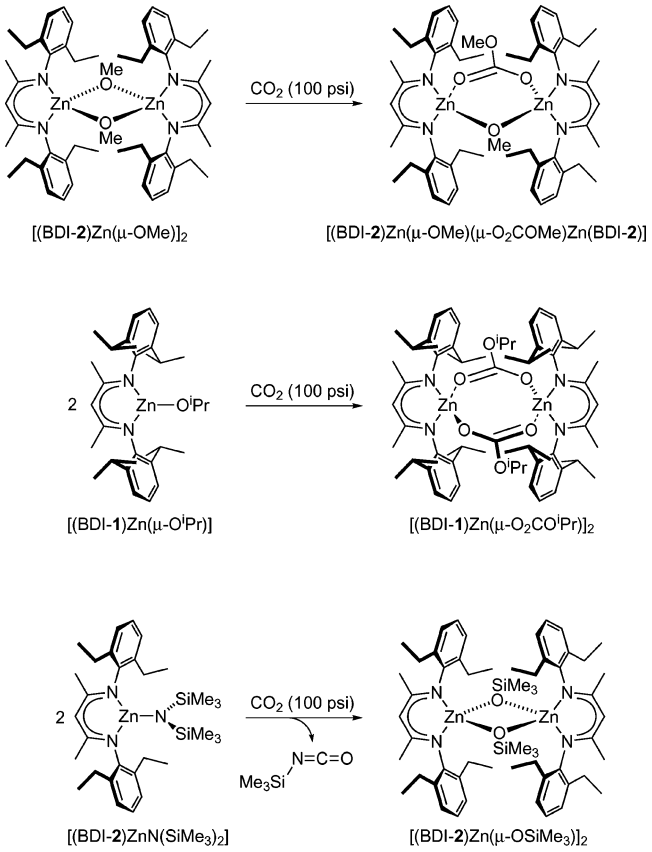

catalytic cycle by reacting with CHO. CO_2 is an unreactive compound whereas epoxides possess significant ring strain. Therefore, we initially predicted the rate-determining step in the copolymerization to be the insertion of CO_2 into the zinc alkoxide bond (Figure 10; Scheme 2). Consequently, the reaction

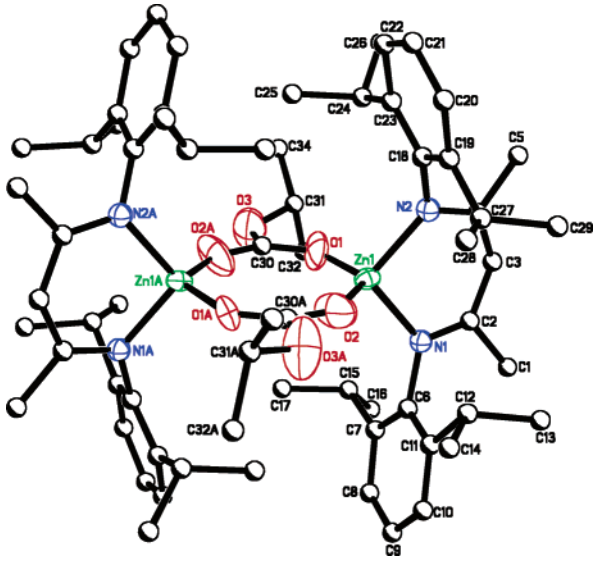

Figure 8. ORTEP drawing of [(BDI-**1**)Zn(μ,η^2-O_2CO^{i}Pr)]$_2$ (non-hydrogen atoms) with thermal ellipsoids drawn at the 40% probability level. Selected bond lengths (Å) and bond angles (deg): Zn(1)−N(1) 1.97(2), Zn(1)−N(2) 1.96(2), Zn(1)−O(1) 2.027(8), Zn(1)−O(2) 1.939(8), O(1)−C(30) 1.23(1), O(2)−C(30A) 1.19(1), O(3)−C(30) 1.39(1), O(1)−Zn(1)−O(2) 126.9(3), N(1)−Zn(1)−N(2) 99.8(3), N(1)−Zn(1)−O(2) 109.7(9), N(2)−Zn(1)−O(1) 102.7(9), C(30)−O(1)−Zn(1) 131.9(8), O(1)−C(30)−O(2A) 137(1).

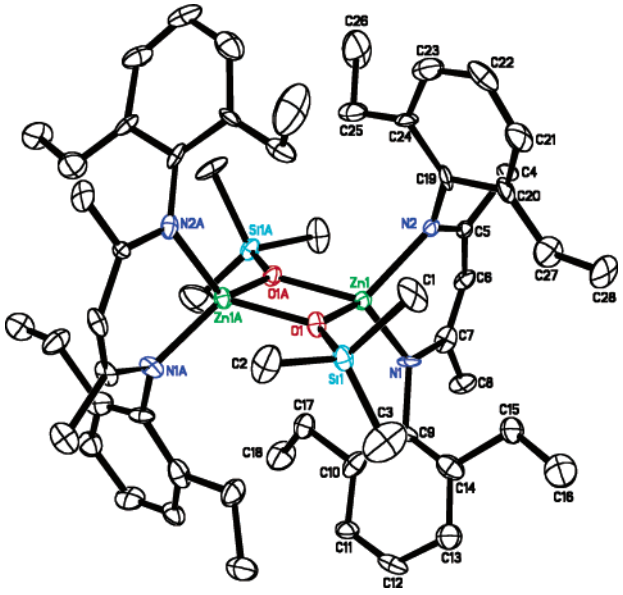

Figure 9. ORTEP drawing of [(BDI-**2**)Zn(μ-OSiMe$_3$)]$_2$ (non-hydrogen atoms) with thermal ellipsoids drawn at the 40% probability level. Selected bond lengths (Å) and bond angles (deg): Zn(1)−N(1) 1.964(8), Zn(1)−N(2) 2.052(8), Zn(1)−O(1) 1.978(2), Zn(1)−O(1A) 2.026(2), O(1)−Si(1) 1.641(2), O(1)−Zn(1)−O(1A) 83.97(8), N(1)−Zn(1)−N(2) 94.7(1), N(1)−Zn(1)−O(1) 124.6(3), N(2)−Zn(1)−O(1A) 115.1(3), Zn(1)−O(1)−Zn(1A) 96.03(8).

of zinc acetates with CHO was anticipated to be extremely fast. By ^{1}H NMR spectroscopy, [(BDI-**1**)ZnOAc]$_2$ only partially reacted with excess CHO over the course of days at 50 °C to give the ring-opened product (Scheme 5). Upon crystallization, only starting material was isolated. We postulated that the $\Delta G°$ of the reaction might be near zero and decided to study the microscopic reverse of this process. ^{1}H NMR spectroscopy showed that the addition of *trans*-2-acetoxycyclohexanol to a solution of (BDI-**1**)ZnN(SiMe$_3$)$_2$ gave a product with resonances

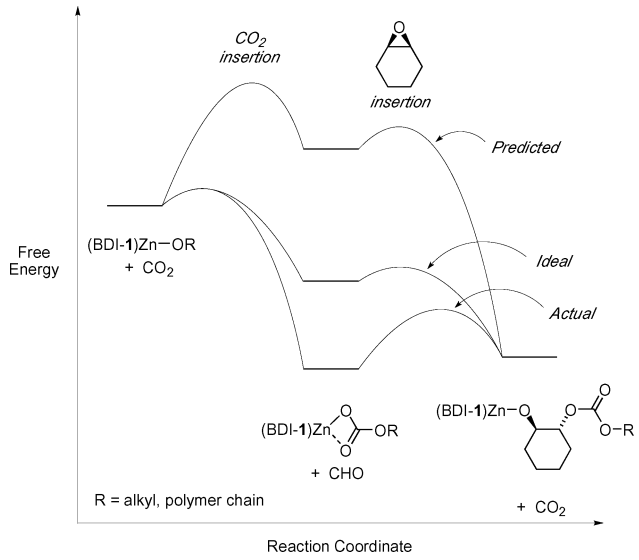

Figure 10. Qualitative energy profiles for insertion of CO_2 and CHO.

consistent with those of (BDI-**1**)ZnOCyOAc, which over 2 days formed [(BDI-**1**)ZnOAc]$_2$ and CHO. By elimination of CHO, the microscopic reverse process occurred, indicating the reaction of CHO with [(BDI-**1**)ZnOAc]$_2$ is an unexpected equilibrium process under these conditions (see Figure 10).

Ideally, the most efficient catalysts would react with both CO_2 and CHO with low activation barriers and negative $\Delta G°$ values (see Figure 10). On the basis of our extensive copolymerization studies with a variety of BDI zinc complexes,[55] we decided to investigate the insertion of CHO into more reactive zinc acetate compounds. [(BDI-**7**)ZnOAc]$_2$, a much more active catalyst than [(BDI-**1**)ZnOAc]$_2$ (see Table 2 for polymerization data), reacted with a slight excess of CHO to yield a new product over the course of several days at room temperature (see Scheme 5). Upon crystallization, the solid-state structure revealed the mono-CHO inserted product, [(BDI-**7**)Zn(μ,η^2-OAc)(μ,η^1-OCyOAc)Zn(BDI-**7**)] (Figure 11; Table 1). The dimeric compound exhibits a distorted tetrahedral geometry around both zinc centers, and the Zn··Zn separation is 3.28 Å. The unreacted acetate bridge is intermediate between *anti-syn* and *syn-syn* geometries such that the O(1)−C(1) acetate bond is twisted out of the plane defined by Zn(1), O(3), and Zn(2) by 29.5°. On the basis of the elongated separation of 3.17 Å between O(4) and Zn(2) and the lack of distortion to a trigonal-bipyramidal geometry around zinc, no dative bond is observed between the reacted acetate moiety and Zn(2). In addition, [(BDI-**7**)Zn(μ,η^2-OAc)(μ,η^1-OCyOAc)Zn(BDI-**7**)] did not react with additional equivalents of CHO over the course of 7 days, although it did react rapidly with CO_2 to complete one full cycle in the alternating copolymerization of CHO and CO_2. Therefore, we

Scheme 5. Insertion Reactions of Cyclohexene Oxide (CHO)

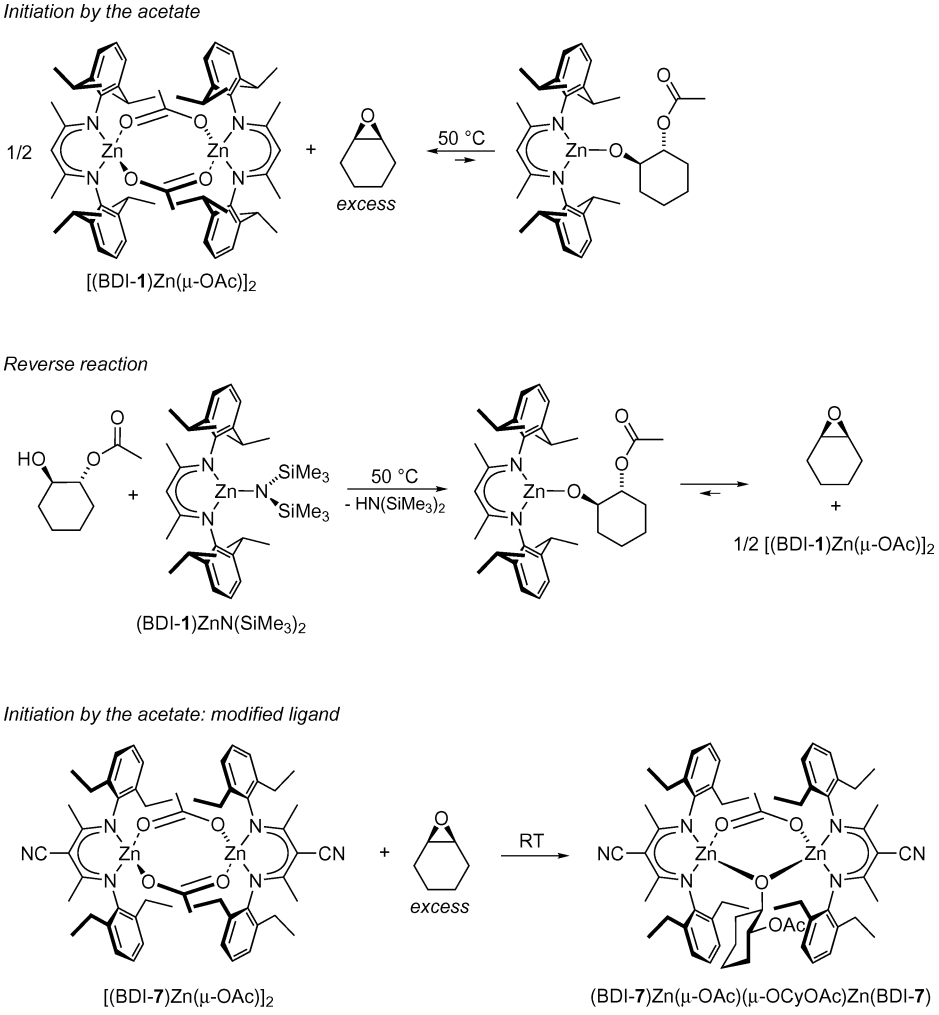

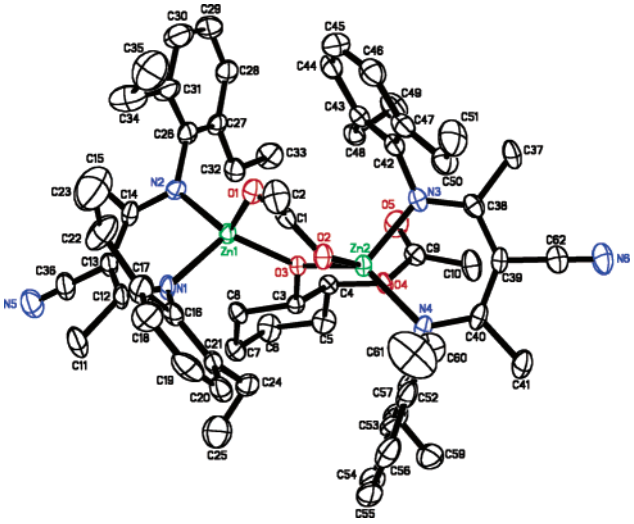

Figure 11. ORTEP drawing of [(BDI-**7**)Zn(μ,η^2-OAc)(μ,η^1-OCyOAc)-Zn(BDI-**7**)] (non-hydrogen atoms) with thermal ellipsoids drawn at the 40% probability level. Selected bond lengths (Å) and bond angles (deg): Zn-(1)−N(1) 2.006(5), Zn(1)−N(2) 1.993(4), Zn(1)−O(1) 1.977(4), Zn(1)−O(3) 1.951(3), Zn(2)−O(2) 2.007(4), Zn(2)−O(3) 1.951(3), O(1)−C(1) 1.254(7), O(1)−Zn(1)−O(3) 104.2(2), O(2)−Zn(2)−O(3) 100.4(2), N(1)−Zn(1)−N(2) 96.1(2), N(1)−Zn(1)−O(3) 118.5(2), N(2)−Zn(1)−O(1) 113.3-(2), Zn(1)−O(3)−Zn(2) 113.1(2), C(1)−O(1)−Zn(1) 120.7(4), C(1)−O(2)−Zn(2) 125.7(4).

propose that the rate-determining step in the copolymerization is actually the insertion of CHO into a zinc carbonate bond. Theoretical molecular orbital studies on the alternating copolymerization mechanism of cyclohexene oxide and CO_2 using monomeric (BDI-**1**)ZnOMe also predict that the rate-determining step is insertion of CHO into a zinc carbonate bond.[68] In addition, [(BDI-**1**)ZnOAc] did not react with CO_2. Finally, it must be noted that like their precursors, the mimics for the presumed intermediates in the copolymerization, including [(BDI-**2**)Zn(μ-OMe)(μ,η^2-OAc)Zn(BDI-**2**)], [(BDI-**2**)Zn(μ-OMe)-(μ,η^2-O_2COMe)Zn(BDI-**2**)], [(BDI-**2**)Zn(μ-OSiMe$_3$)]$_2$, and [(BDI-**7**)Zn(μ,η^2-OAc)(μ,η^1-OCyOAc)Zn(BDI-**7**)] but with the exception of the insoluble [(BDI-**1**)Zn(μ,η^2-O_2CO^{i}Pr)]$_2$, are highly active for the alternating copolymerization of CHO and CO_2. Furthermore, they have similar TOFs and yield monodisperse polycarbonate with low PDIs.

Rate Studies of the Alternating Copolymerization of CHO and CO_2. In Table 2, copolymerization data of monomeric (BDI)ZnN(SiMe$_3$)$_2$ complexes[54] with ligands **1** and **2** are reported. (BDI-**1**)ZnN(SiMe$_3$)$_2$ and (BDI-**2**)ZnN(SiMe$_3$)$_2$ produced polycarbonate with similar activities (TOF ≈ 350 h^{-1}) in a 30-min polymerization. The polycarbonate possessed greater than 94% carbonate linkages, similar molecular weights (M_n ≈ 25,000), and low PDIs (PDI = 1.10−1.16). Interestingly, when equimolar amounts of (BDI-**1**)ZnN(SiMe$_3$)$_2$ and (BDI-**2**)ZnN-(SiMe$_3$)$_2$ were simultaneously exposed to cyclohexene oxide and 100 psi CO_2 in a one-pot reaction, such that the reaction conditions and total zinc concentration were unchanged, a doubling of activity (TOF = 658 h^{-1}) resulted (Scheme 6). The polycarbonate produced possessed 94% carbonate linkages, a M_n of 40,800 g/mol, and a unimodal PDI of 1.17. This result suggests that two zinc centers are interacting during the

Scheme 6. Effect of Catalyst Combinations on Rate

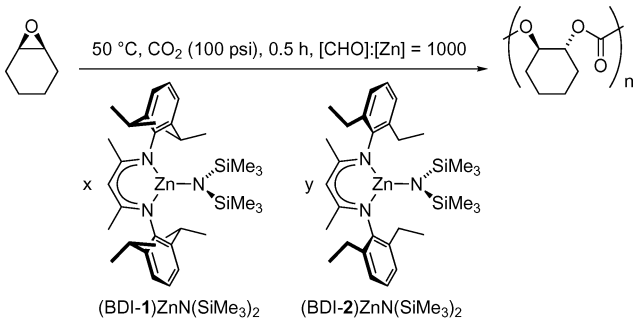

x:y	TOF (h^{-1})
1.0:0	345
0:1.0	358
0.5:0.5	658

copolymerization via formation of mixed (BDI-**1**) and (BDI-**2**) zinc active species.

Table 2 also shows polymerization data for [(BDI)ZnOAc] complexes using ligands **1**−**7**. [(BDI-**3**)ZnOAc]$_2$ exhibited no polymerization activity, which we attribute to the tightly bound dimeric state of the complex.[54] Polymerization activity emerges as the steric bulk on the *N*-aryl rings is increased. [(BDI-**2**)-ZnOAc]$_2$ copolymerized CHO and CO_2 (100 psi) at 50 °C to give a TOF of 431 h^{-1} in a 30-min polymerization. [(BDI-**4**)-ZnOAc]$_2$, which has *para tert*-butyl substituents on the 2,6-diethylaniline moieties, elicited a further augmentation of activity to 622 h^{-1}. The unsymmetrical [(BDI-**5**)ZnOAc]$_2$ is the most active catalyst of the six (Figure 12) as it produced polycarbonate with a TOF of 729 h^{-1}. As the substituents on the *ortho* positions continue to increase in size, the polymerization activity suffers. [(BDI-**1**)ZnOAc]$_2$ produced poly(cyclohexene carbonate) with a TOF of 360 h^{-1}. Finally, the addition of *para tert*-butyl substituents to the diisopropyl aniline moiety on [(BDI-**6**)ZnOAc]$_2$ causes a dramatic decrease in polymerization activity to only 28 h^{-1} over 5 h.[69] As shown in Figure 12, the polymerization activity peaks with the [(BDI-**5**)ZnOAc]$_2$ and declines as qualitative steric bulk is decreased or increased on the zinc catalyst. We propose [(BDI-**5**)ZnOAc]$_2$ contains enough steric bulk to be a very reactive dimeric initiator. Both [(BDI-**1**)ZnOAc] and [(BDI-**6**)ZnOAc] show reduced activities due to excessive steric bulk. Therefore, [(BDI-**5**)ZnOAc]$_2$ possesses an optimal ligand arrangement to catalyze the copolymerization of CHO and CO_2 effectively.

A proposed mechanism must account for several intriguing observations: (1) the doubling of activity observed in the copolymerization by (BDI-**1**)ZnN(SiMe$_3$)$_2$ and (BDI-**2**)ZnN-(SiMe$_3$)$_2$ mixtures; (2) large activity differences for a series of structurally related compounds; (3) the profound effect of adding *para tert*-butyl groups to the catalysts; and (4) the exclusive insertion of one CHO monomer unit per two zinc centers in the case of [(BDI-**7**)ZnOAc]$_2$. We considered that the BDI zinc centers do not act independently but rather in a cooperative, bimetallic fashion.[55] A bimetallic mechanism satisfies all of these observations: (1) CO_2 insertion into the monomeric (BDI-**1**)ZnN(SiMe$_3$)$_2$ and (BDI-**2**)ZnN(SiMe$_3$)$_2$ can form more acti-

(68) Liu, Z. W.; Torrent, M.; Morokuma, K. *Organometallics* **2002**, *21*, 1056−1071.

(69) We are currently investigating the origin of the bimodal GPC traces of the polymer produced using [(BDI-**6**)ZnOAc] (see Table 2). Preparatory GPC of the polymer shows the high molecular weight peak to be predominantly polyether, whereas the low molecular weight fraction is primarily polycarbonate.

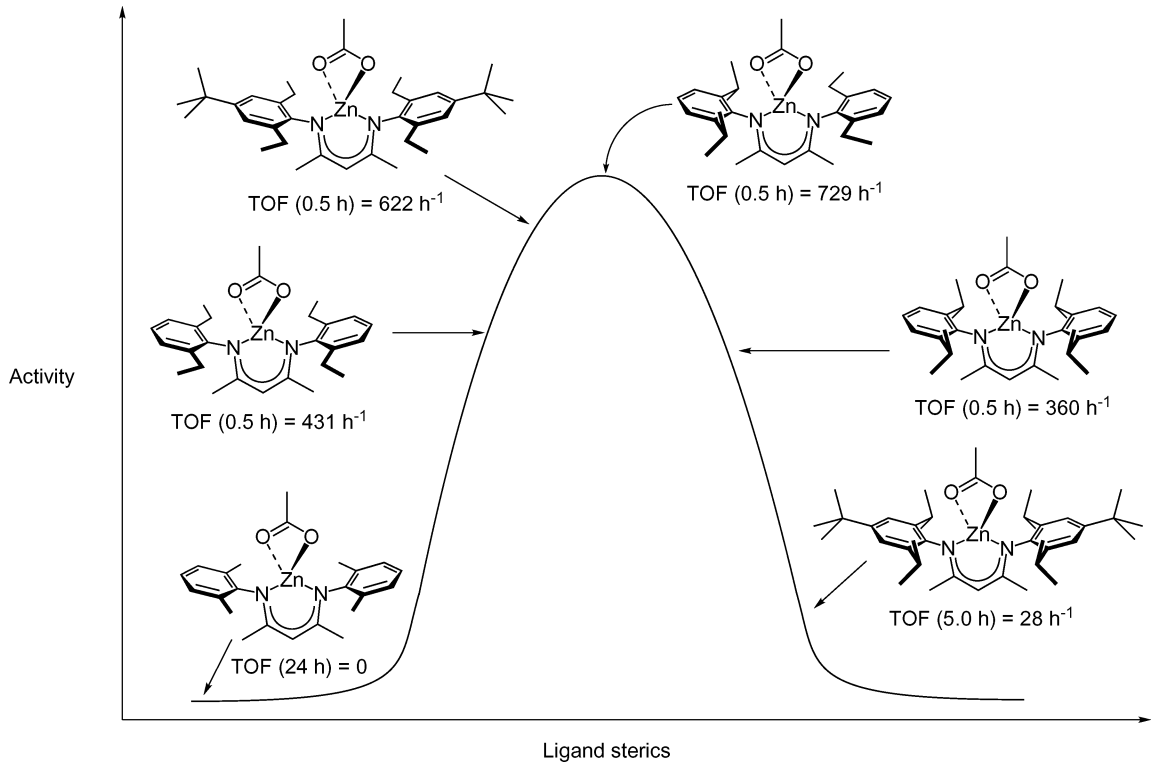

Figure 12. Activity versus qualitative ligand sterics for (BDI)ZnOAc catalysts. Copolymerization of neat CHO ([CHO]:[Zn] = 1000, 100 psi CO_2, T_{rxn} = 50 °C).

vated (BDI-**1**)Zn/(BDI-**2**)Zn mixed catalytic species; (2) tightly bound dimers do not allow coordination of and reaction with CHO or CO_2, whereas sterically encumbered monomeric species cannot easily access a bimetallic transition state; (3) molecular modeling suggests that *para tert*-butyl substituents do impede access to a bimetallic transition state, but do not affect a monometallic enchainment; and (4) CHO insertion requires a dimeric zinc species with two bridging μ,η^2-O_2CR or μ,η^2-O_2-COR groups (R = alkyl, growing polymer chain) capable of attacking the epoxide, and [(BDI-**7**)Zn(μ,η^2-OAc)(μ,η^1-OCyOAc)-Zn(BDI-**7**)] lacks this requirement.

Bimetallic mechanisms have been widely observed in synthetic catalytic processes as well as natural ones. For instance, aminopeptidases, phosphatases, and phosphotriesterases are just a few examples of natural enzymatic systems that benefit from two zinc centers at the active site of the enzyme.[70] Scientists have tried to mimic the successful strategy of nature to harness the benefits of cooperative bimetallic mechanisms.[71,72] Several organic transformations are presumed to occur via bimetallic metal centers, including asymmetric aldol condensations,[73] ring-opening of epoxides,[74,75] and homopolymerization of epoxides.[76] Bi- or multimetallic active species have also been proposed in epoxide/CO_2 coupling reactions.[77]

Solution dynamics, stoichiometric initiation steps, and copolymerization rates of BDI zinc complexes all strongly suggest that a bimetallic mechanism is indeed in operation in the alternating copolymerization of CHO and CO_2; however, kinetic studies were performed to directly monitor the copolymerization.[55] In situ IR[78] determines the rate of polycarbonate

(70) For reviews on cooperative bimetallic catalysis in enzymatic systems, see: (a) Cricco, J. A.; Orellano, E. G.; Rasia, R. M.; Ceccarelli, E. A.; Vila, A. *J. Coord. Chem. Rev.* **1999**, *192*, 519−535. (b) Wilcox, D. E. *Chem. Rev.* **1996**, *96*, 2435−2458. (c) Lipscomb, W. N.; Strater, N. *Chem. Rev.* **1996**, *96*, 2375−2433. (d) Coleman, J. E. *Curr. Opin. Chem. Biol.* **1998**, *2*, 222−234. (e) Strater, N.; Lipscomb, W. N.; Klabunde, T.; Krebs, B. *Angew. Chem., Int. Ed. Engl.* **1996**, *35*, 2024−2055. (f) Steinhagen, H.; Helmchen, G. *Angew. Chem., Int. Ed. Engl.* **1996**, *35*, 2339−2342.

(71) For an example of biomimetic, bimetallic catalyst design for lactone polymerization, see: Williams, C. K.; Brooks, N. R.; Hillmyer, M. A.; Tolman, W. B. *Chem. Commun*. **2002**, 2132−2133.

(72) For a review on synthetic bimetallic catalysts as enzymatic mimics, see: van den Beuken, E. K.; Feringa, B. L. *Tetrahedron* **1998**, *54*, 12985−13011.

(73) For references on asymmetric aldol condensation using bimetallic zinc compounds, see the following and references within: (a) Kitamura, M.; Okada, S.; Suga, S.; Noyori, R. *J. Am. Chem. Soc.* **1989**, *111*, 4028−4036. (b) Kitamura, M.; Suga, S.; Niwa, M.; Noyori, R. *J. Am. Chem. Soc.* **1995**, *117*, 4832−4842. (c) Kitamura, M.; Suga, S.; Oka, H.; Noyori, R. *J. Am. Chem. Soc.* **1998**, *120*, 9800−9809. (d) Trost, B. M.; Ito, H. *J. Am. Chem. Soc.* **2000**, *122*, 12003−12004. (e) Trost, B. M.; Silcoff, E. R.; Ito, H. *Org. Lett.* **2001**, *3*, 2497−2500. (f) Rasmussen, T.; Norrby, P. O. *J. Am. Chem. Soc.* **2001**, *123*, 2464−2465. (g) Pu, L.; Yu, H. B. *Chem. Rev.* **2001**, *101*, 757−824.

(74) For asymmetric ring-opening of epoxides using Cr or Co salen complexes, see the following and references within: (a) Jacobsen, E. N. *Acc. Chem. Res.* **2000**, *33*, 421−431. (b) Ready, J. M.; Jacobsen, E. N. *Angew. Chem., Int. Ed.* **2002**, *41*, 1374−1377. (c) Schaus, S. E.; Brandes, B. D.; Larrow, J. F.; Tokunaga, M.; Hansen, K. B.; Gould, A. E.; Furrow, M. E.; Jacobsen, E. N. *J. Am. Chem. Soc.* **2002**, *124*, 1307−1315. (d) Ready, J. M.; Jacobsen, E. N. *J. Am. Chem. Soc.* **2001**, *123*, 2687−2688. (e) Konsler, R. G.; Karl, J.; Jacobsen, E. N. *J. Am. Chem. Soc.* **1998**, *120*, 10780−10781. (f) Hansen, K. B.; Leighton, J. L.; Jacobsen, E. N. *J. Am. Chem. Soc.* **1996**, *118*, 10924−10925.

(75) For Zr-catalyzed enantioselective ring-opening of epoxides, see the following: (a) Nugent, W. A. *J. Am. Chem. Soc*. **1998**, *120*, 7139−7140. (b) McCleland, B. W.; Nugent, W. A.; Finn, M. G. *J. Org. Chem.* **1998**, *63*, 6656−6666.

(76) For studies where a bimetallic epoxide enchainment mechanism is proposed, see the following and references within: (a) Vandenberg, E. J. *J. Polym. Sci*. **1960**, *47*, 486-489. (b) Price, C. C.; Spector, R. *J. Am. Chem. Soc*. **1966**, *88*, 4171−4173. (c) Osgan, M.; Teyssie, P. *J. Polym. Sci. Part B: Polym. Lett*. **1967**, *5*, 789−792. (d) Vandenberg, E. J. *J. Polym. Sci., Part A: Polym. Chem*. **1986**, *24*, 1423−1431. (e) Watanabe, Y.; Yasuda, T.; Aida, T.; Inoue, S. *Macromolecules* **1992**, *25*, 1396−1400. (f) Sugimoto, H.; Kawamura, C.; Kuroki, M.; Aida, T.; Inoue, S. *Macromolecules* **1994**, *27*, 2013−2018. (g) Chisholm, M. H.; Navarro-Llobet, D.; Simonsick, W. J. *Macromolecules* **2001**, *34*, 8851−8857. (h) Braune, W.; Okuda, J. *Angew. Chem., Int. Ed*. **2003**, *42*, 64−68. To the best of our knowledge, no kinetic studies have been performed on these systems. However, Inoue has reported kinetic studies for the ring-opening polymerization of δ-valerolactone that illustrate a second-order dependence in aluminum porphyrin alcoholates. See: Shimasaki, K.; Aida, T.; Inoue, S. *Macromolecules* **1987**, *20*, 3076−3080.

formation through the emerging carbonyl stretch (approximately 1750 cm^{-1}).[17,18,79,80] To determine the rate law, we measured reaction orders in all three components of the polymerization[62,81] (eq 1):

$$d[P]/dt = k_p[CHO]^x[CO_2]^y[Zn]_{tot}^{\ z} \quad (1)$$

On the basis of stoichiometric initiation reactions, we believed CHO insertion would be rate-determining (first-order), whereas CO_2 insertion would be a fast step and would thereby not be included in the rate equation for the polymerization. The copolymerization of CHO (1.98 M in toluene) and CO_2 from 50 to 200 psi was performed using [(BDI-**5**)ZnOAc] (9.88 mM in total Zn) at 30 °C and [(BDI-**2**)ZnOAc] (15.4 mM in total Zn) at 50 °C. Zeroth-order kinetics in CO_2 monomer were observed by monitoring initial rates (up to 15% conversion).[62] Initial rates for [(BDI-**5**)ZnOAc] and [(BDI-**2**)ZnOAc] were approximately 0.025 and 0.008 abs_{CO}/min (the carbonyl absorbance, abs_{CO}, is directly proportional to [polycarbonate]), respectively.[62,82] Surprisingly, polycarbonate was synthesized with pressures as low as 20 psi CO_2 using [(BDI-**5**)ZnOAc]. This is an unprecedented result, as previously reported polymerization systems require much higher pressures of CO_2.[83] At 20 psi, the rate of backbiting competes with CO_2 insertion into the growing polymer chain, producing a small amount of *trans*-cyclohexenecarbonate (approximately 3% by ^{1}H NMR spectroscopy). Given the zero-order dependence in CO_2, the overall rate law was simplified to eq 2:

$$d[P]/dt = k_p[CHO]^x[CO_2]^0[Zn]_{tot}^{\ z} \quad (2)$$

where k_p is the propagation rate constant. To determine the order in epoxide monomer (x), various concentrations of CHO (0.82−3.29 M in toluene) were copolymerized with 300 psi CO_2 using [(BDI-**1**)ZnOAc] (13.9 mM in total Zn) at 30 °C.[62] As expected, the polycarbonate carbonyl stretch intensities increased with higher CHO concentrations. The initial rates for each run were plotted versus [CHO], demonstrating a first-order dependence on monomer concentration.[62] Therefore, the rate-determining step is indeed the insertion of CHO into a growing carbonate species. The polymerization proceeds as shown in eq 3:

$$d[P]/dt = k_{obs}[CHO]^1 \quad (3)$$

where $k_{obs} = k_p[Zn]_{tot}^{\ z}$. To ascertain the order in total zinc, $[Zn]_{tot}$, the copolymerization of 1.98 M CHO in toluene and 300 psi CO_2 was completed using [(BDI-**1**)ZnOAc] (3.87−13.4 mM in total Zn) at 30 °C and 50 °C. By plotting ln k_{obs} versus ln $[Zn]_{tot}$, orders in total zinc of 1.39 ± 0.04 and 1.73 ± 0.06 were discovered at 30 and 50 °C (Figure 13), respectively. Therefore, the copolymerization of CHO and CO_2 using [(BDI-**1**)ZnOAc] at 50 °C exhibited the following overall rate law:

$$d[P]/dt = k_p[CHO]^1[CO_2]^0[Zn]_{tot}^{\ 1.73} \quad (4)$$

Furthermore, the copolymerization of 1.98 M CHO in toluene and 300 psi CO_2 was investigated using [(BDI-**5**)ZnOAc] (1.04−9.88 mM in total Zn) at 30 and 50 °C. By plotting ln k_{obs} versus ln $[Zn]_{tot}$, orders in total zinc of 1.37 ± 0.02 and 1.83 ± 0.04 were discovered at 30 and 50 °C (Figure 13), respectively. Figure 14 illustrates a plot of initial rate versus $[Zn]_{tot}$ at 50 °C, which clearly shows a higher order dependence in [(BDI-**5**)ZnOR], where R is alkyl, acyl, or polymer chain.

Orders in total zinc that approach 2 are most logically explained by a bimetallic transition state for epoxide ring opening and a predominantly monomeric (BDI)ZnO_2COR ground state. We attribute the increase in order for both [(BDI-**1**)ZnOAc] and [(BDI-**5**)ZnOAc] at higher temperatures to a greater proportion of [(BDI)ZnO_2COR] in the monomeric (M) state (Figure 15). Dynamic solution studies (monomer/dimer equilibrium) of [(BDI-**1**)ZnOAc] show an increase in the concentration of the monomeric form of the complex as the temperature rises. Hence, if a bimetallic mechanism is operating, a higher percentage of monomeric ground state would *increase* the order in [(BDI)ZnO_2COR] at higher temperatures. The rate law for CHO/CO_2 copolymerization is a summation of five possible elementary steps, as shown in Figure 15. Although there are multiple possible bimetallic transition structures that accommodate the near second order in total zinc, we currently favor the one in Figure 15.

Even though rate studies indicate the dominance of a bimetallic mechanism, we attempted to collect more information to probe the possibility of a mixture of monometallic and bimetallic transition states. If a monometallic transition state exclusively operates, the rate of a catalyst that exists as a dimer in the ground state would theoretically exhibit an order in zinc dimer (D) of 0.5. Conversely, if only a bimetallic transition state occurs, the rate of the same dimeric catalyst would show an order in zinc dimer (D) of 1.0. Finally, the zinc centers of a dimeric catalyst may act independently; this will exhibit the same kinetics. Because [(BDI-**2**)ZnOAc] is solely dimeric by ^{1}H NMR spectroscopy, even at elevated temperatures of 100 °C, we investigated its kinetics for the alternating copolymerization of CO_2 and CHO. The copolymerization of 1.98 M CHO in toluene and 300 psi CO_2 was completed using

(77) See refs 12, 22, 24, 27−30, 55 and the following: (a) Kobayashi, M.; Inoue, S.; Tsuruta, T. *Macromolecules* **1971**, *4*, 658−659. (b) Inoue, S.; Kobayashi, M.; Koinuma, H.; Tsuruta, T. *Makromol. Chem.* **1972**, *155*, 61−73. (c) Kobayashi, M.; Inoue, S.; Tsuruta, T. *J. Polym. Sci.: Polym. Chem. Ed.* **1973**, *11*, 2383−2385. (d) Kobayashi, M.; Tang, Y. L.; Tsuruta, T.; Inoue, S. *Makromol. Chem.* **1973**, *169*, 69−81. (e) Kuran, W.; Pasynkiewicz, S.; Skupinska, J.; Rokicki, A. *Makromol. Chem. Macromol. Chem. Phys.* **1976**, *177*, 11−20. (f) Kuran, W. *Appl. Organomet. Chem.* **1991**, *5*, 191−194. (g) Kuran, W.; Listos, T. *Macromol. Chem. Phys.* **1994**, *195*, 1011−1015.

(78) ASI Applied Systems, Millersville, MD 21108.

(79) In all kinetic studies, the resultant polycarbonates contain >99% carbonate linkages as determined by ^{1}H NMR spectroscopy. In addition, the polycarbonates possess molecular weights based on [CHO]:[Zn] and PDIs are approximately 1.1, as determined by gel permeation chromatography (calibrated with polystyrene standards in tetrahydrofuran). It should be noted that higher levels of carbonate linkages are found in polycarbonate synthesized in toluene solution versus neat CHO. A similar phenomenon has been observed in ref 17.

(80) For some examples of in situ IR studies, see: (a) Rutherford, J. L.; Hoffmann, D.; Collum, D. B. *J. Am. Chem. Soc.* **2002**, *124*, 264−271. (b) Sun, X. F.; Collum, D. B. *J. Am. Chem. Soc.* **2000**, *122*, 2452−2458. (c) Lucht, B. L.; Collum, D. B. *J. Am. Chem. Soc.* **1995**, *117*, 9863−9874. (d) Bernstein, M. P.; Collum, D. B. *J. Am. Chem. Soc.* **1993**, *115*, 8008−8018. (e) Allmendinger, M.; Eberhardt, R.; Luinstra, G.; Rieger, B. *J. Am. Chem. Soc.* **2002**, *124*, 5646−5647.

(81) The concentration of BDI zinc complexes, [(BDI)ZnOR] or $[Zn]_{tot}$, although expressed in units of molarity, refers to the concentration of the monomer unit (normality). However, note that in solution, $[Zn]_{tot} = 2[D] + [M]$, where D = dimer and M = monomer.

(82) Higher CO_2 pressures (approximately 200 psi CO_2 and above) cause slightly decreased initial rates, which we attribute to a dilution of epoxide. Furthermore, control experiments show lower carbonyl absorbance levels as CO_2 pressure is increased (see Supporting Information). Therefore, we have adjusted the initial rate values to account for these decreased absorbance levels.

(83) For leading references employing catalyst systems under high pressures of CO_2 or supercritical CO_2, see refs 8−21.

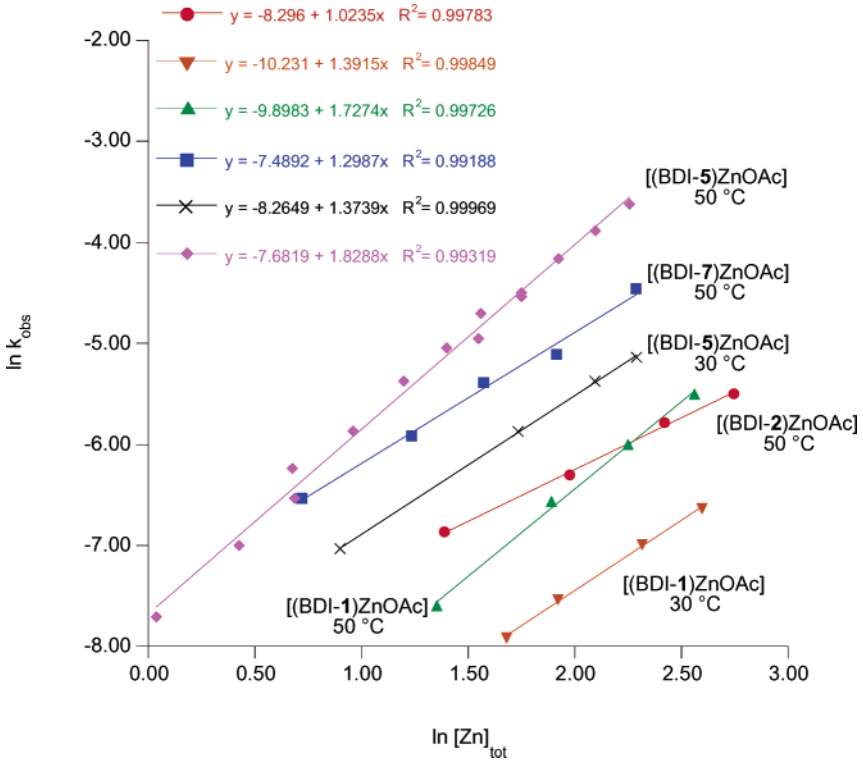

Figure 13. Copolymerization of CHO (1.98 M in toluene) + CO_2 (300 psi) using [(BDI)ZnOAc] catalysts.

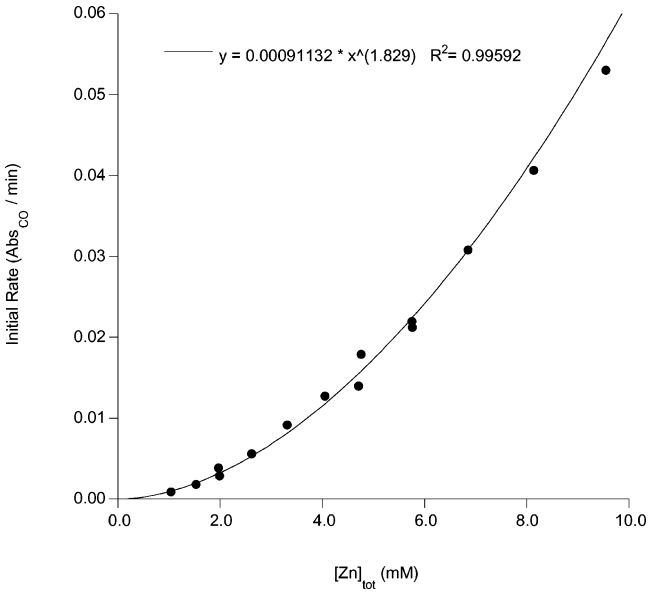

Figure 14. Initial rates of the copolymerization of CHO (1.98 M in toluene) + CO_2 (300 psi) using [(BDI-**5**)ZnOAc] at 50 °C.

[(BDI-**2**)ZnOAc] (4.01−15.6 mM in total Zn) at 50 °C. By plotting ln k_{obs} versus ln $[Zn]_{tot}$, an order in total zinc of 1.02 ± 0.03 was determined (see Figure 13). A plot of initial rate versus $[Zn]_{tot}$ for the polymerization reactions using [(BDI-**1**)ZnOAc] and [(BDI-**2**)ZnOAc] at 50 °C demonstrates an order in total zinc that is 1 for [(BDI-**2**)ZnOAc] and greater than 1 for [(BDI-**1**)ZnOAc] (Figure 16).

Rate studies were also performed on [(BDI-**7**)ZnOAc] to probe the effect of the electron-withdrawing cyano substituent. The copolymerization of 1.98 M CHO in toluene and 300 psi CO_2 was investigated using [(BDI-**7**)ZnOAc] (2.06−9.86 mM in total Zn) at 50 °C. By plotting ln k_{obs} versus ln $[Zn]_{tot}$, an order in total zinc of 1.30 ± 0.07 was determined (see Figure 13). We interpret this to mean that a more significant proportion of monomeric ground state persists with [(BDI-**7**)ZnOAc] than with [(BDI-**2**)ZnOAc]. We propose that electron withdrawal by the cyano substituent increases the electrophilicity of [(BDI)-ZnOR] and thereby facilitates the coordination of CHO. The accumulated rate data demonstrate orders in total zinc from 1.02 to 1.83, which vary due to temperature and steric and electronic influences of the catalyst. These factors also directly affect solution behavior and copolymerization activities. As sterics and/or temperature increase, the proportion of monomeric complex in solution, and, accordingly, the order in total zinc, rise. As groups on the ligand framework become too bulky, however, activity suffers due to a monomeric species that struggles to access a bimetallic transition state. Catalysts that can attain a loose dimeric ground state have kinetic advantages over their monomeric or strongly dimerized counterparts.

Scheme 7 shows the proposed mechanism for the alternating copolymerization of CHO and CO_2 using BDI zinc complexes based on our copolymerization activities and rate data, dynamic solution studies, and insight into the enchainment steps. The zinc alkoxide monomer (**A**) or dimer ($\mathbf{A_2}$) inserts CO_2 to yield either carbonate complexes (**B**, $\mathbf{B_2}$) or an alkoxide/carbonate dimer (**AB**), depending on relative sterics and propagating groups. $\mathbf{A_2}$, **A**, and **AB** compounds do not react with CHO. The dimeric eight-membered carbonate dimer ($\mathbf{B_2}$) mimics [(BDI)-ZnOAc]$_2$ compounds, which with adequate bulk (e.g., [(BDI-**1**)Zn(μ-OAc)]), participate in a monomer/dimer equilibrium. $\mathbf{B_2}$ reacts with CHO in an equilibrium process (e.g., [(BDI-**1**)Zn-(μ-OAc)]$_2$) or cleanly (e.g., [(BDI-**7**)Zn(μ-OAc)]$_2$) to **AB**, but **B** and $\mathbf{B_2}$ do not react with CO_2. The *trans* ring-opened product collapses to **AB** (e.g., [(BDI-**7**)Zn(μ,η^2-OAc)(μ,η^1-OCyOAc)-Zn(BDI-**7**)]). **AB** subsequently reacts with CO_2 to complete one full catalytic cycle. This cycle is continually propagated to make

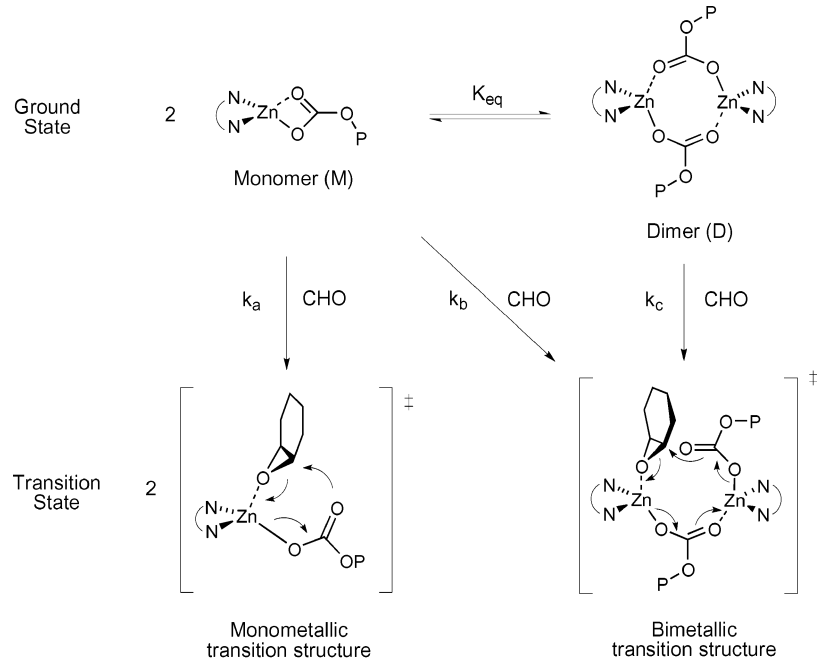

(1) rate = $k_a[CHO]^1[M]^1$
(2) rate = $k_a K_{eq}^{-1/2}[CHO]^1[D]^{1/2}$
(3) rate = $k_b[CHO]^1[M]^2$
(4) rate = $k_c[CHO]^1[D]^1$
(5) rate = $k_c K_{eq}[CHO]^1[M]^2$

Figure 15. Potential ground and transition structures for ring opening of CHO, and the corresponding rate equations for five possible elementary steps. Rate equations (1) and (2) indicate processes that proceed through a monometallic transition state, whereas (3), (4), and (5) show processes that utilize a bimetallic transition state. The observable ground state associated with (1), (3) , and (5) is a monomeric species, whereas the ground state associated with (2) and (4) is a dimeric species.

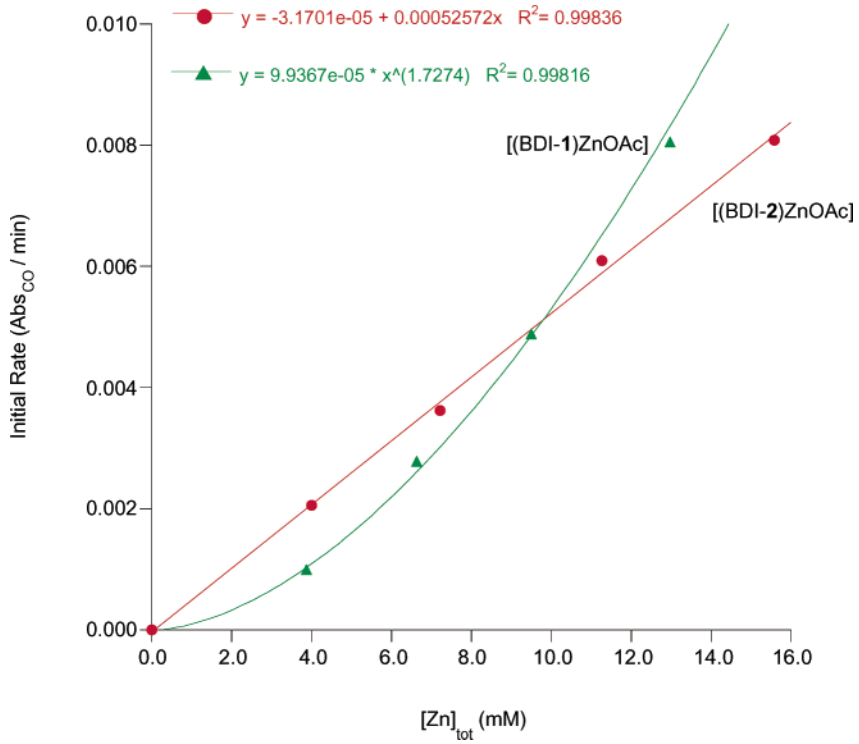

Figure 16. Copolymerization of CHO (1.98 M in toluene) + CO_2 (300 psi) using [BDI-**1**)ZnOAc] and [BDI-**2**)ZnOAc] catalysts at 50 °C.

a polycarbonate chain possessing a molecular weight determined by the ratio of [CHO] to [Zn]. With the aid of rate data, we believe **B** and $\mathbf{B_2}$ both participate as ground state species and access a bimetallic transition state in the rate-determining step of the copolymerization (see Scheme 7). We tentatively propose that one zinc species coordinates and activates the epoxide and

Scheme 7. Proposed Mechanism of Copolymerization (CHO = cyclohexene oxide; P = polymer chain)

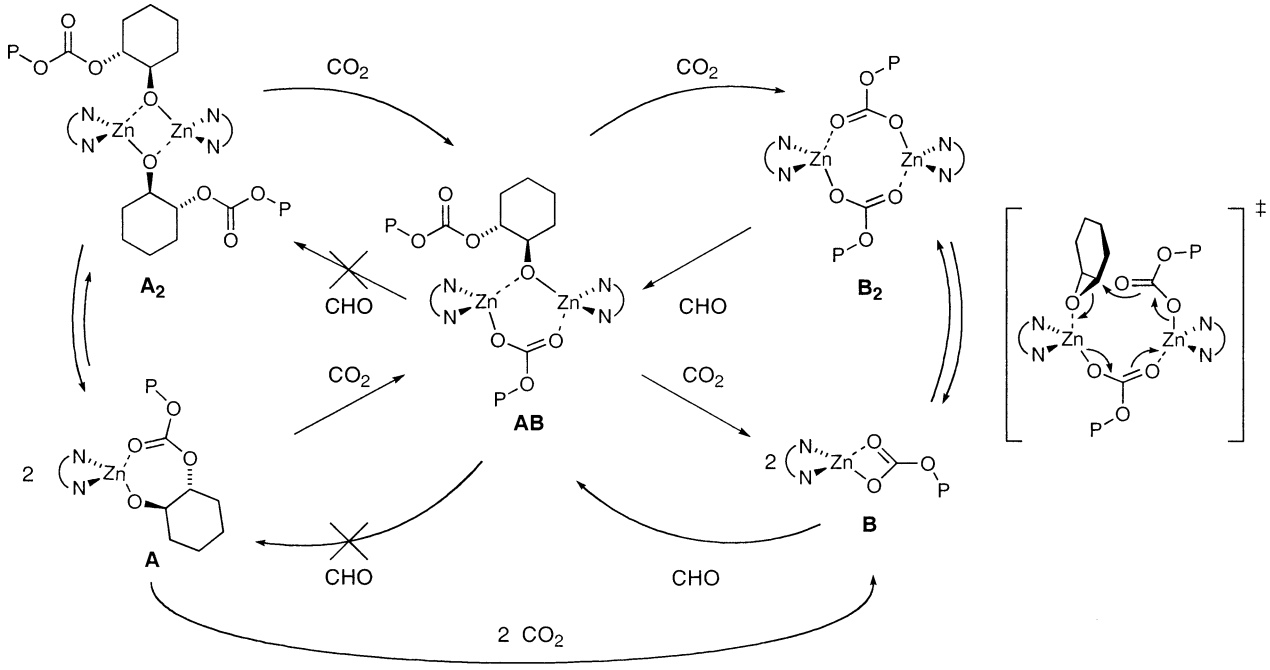

the second zinc species delivers the carbonate propagating species to the back side of the *cis*-epoxide ring in a concerted fashion. The ratio of $\mathbf{B_2}$ to **B** in the ground state changes depending on reaction temperature and steric and electronic factors of the BDI framework, and consequently the orders in zinc are altered.

Conclusion

We have synthesized a wide array of BDI zinc complexes that demonstrate excellent activities for the alternating copolymerization of CHO and CO_2. Dynamic solution studies reveal that sterically hindered zinc acetates, including [(BDI-**1**)Zn(μ-OAc)]$_2$ and [(BDI-**6**)Zn(μ-OAc)]$_2$, participate in monomer/dimer equilibria which demonstrate enthalpic stability toward the dimer. The sterically less impeded [(BDI-**2**)Zn(μ-OAc)]$_2$ and [(BDI-**2**)Zn(μ-OMe)]$_2$ complexes react to from a six-membered ring mixed dimeric species, suggesting the stability of the six-membered ring over the four-membered alkoxides and eight-membered acetate dimers. Stoichiometric enchainment reactions reveal BDI zinc acetates react with CHO and zinc alkoxides react with CO_2. In addition, copolymerization behavior suggests that two zinc centers are interacting in the polymerization. Rate studies were performed on the copolymerization, showing a zero-order dependence in CO_2, a first-order dependence in CHO, and orders in total zinc from 1.0 to 1.8. Variations in ligand sterics, electronics, and temperature play a major role in the order in total zinc. We propose that a bimetallic mechanism is in operation, where sterically hindered zinc complexes, such as [(BDI-**1**)ZnOAc] and [(BDI-**5**)ZnOAc], access a bimetallic transition state through both monomeric and dimeric ground states. Sterically unencumbered zinc complexes, including [(BDI-**2**)ZnOAc], operate via a bimetallic transition state from a completely dimeric ground state. The rate studies support a bimetallic mechanism; however, kinetics do not prove a mechanism. We cannot discount the possibility of minor contribution from a monometallic mechanism. Future work will aim to investigate the possibility of a monometallic transition state and to quantitate the equilibrium constants, thermodynamics, and the activation barriers involved in the insertion processes of zinc alkoxides with CO_2 and zinc acetates with epoxides. Taking the mechanism into account, we will develop new catalysts with improved activities and selectivities. We will also try to understand the importance of the unsymmetrical ligand geometries in facilitating catalytic activities. Finally, we will investigate other monomers, such as propylene oxide, to determine whether a similar bimetallic mechanism is occurring.

Acknowledgment. We thank Professors David Collum and Marc Hillmyer for useful discussions on kinetics and Joseph J. Reczek for the synthesis of 2,6-diethyl-4-*tert*-butylaniline. This work was generously supported by the NSF (CHE-0243605). We also thank the Cornell University Center for Biotechnology, the New York State Center for Advanced Technology supported by the New York State Science and Technology Foundation, and industrial partners for partial support of this research. This research made use of the Cornell Center for Materials Research Shared Experimental Facilities, supported through the National Science Foundation Materials Research Science and Engineering Centers program (DMR-0079992), and the Cornell Chemistry Department X-ray Facility (supported by the NSF; CHE-9700441). G.W.C. gratefully acknowledges an Alfred P. Sloan Research Fellowship, an Arnold and Mabel Beckman Foundation Young Investigator Award, a Camille Dreyfus Teacher-Scholar Award, a Packard Foundation Fellowship in Science and Engineering, and generous support from Eastman Chemical. D.R.M. is grateful for a Corning Foundation Science Fellowship.

Supporting Information Available: Experimental details, including synthetic details, crystal structure data for all complexes, rate studies, and equilibria plots. This material is available free of charge via the Internet at http://pubs.acs.org.

JA030085E